

---

# TPP-SD: Accelerating Transformer Point Process Sampling with Speculative Decoding

---

Anonymous Author(s)

Affiliation

Address

email

## Abstract

1 We propose TPP-SD, a novel approach that accelerates Transformer temporal  
2 point process (TPP) sampling by adapting speculative decoding (SD) techniques  
3 from language models. By identifying the structural similarities between thinning  
4 algorithms for TPPs and speculative decoding for language models, we develop  
5 an efficient sampling framework that leverages a smaller draft model to generate  
6 multiple candidate events, which are then verified by the larger target model  
7 in parallel. TPP-SD maintains the same output distribution as autoregressive  
8 sampling while achieving significant acceleration. Experiments on both synthetic  
9 and real datasets demonstrate that our approach produces samples from identical  
10 distributions as standard methods, but with  $2\text{-}6\times$  speedup. Our ablation studies  
11 analyze the impact of hyperparameters such as draft length and draft model size on  
12 sampling efficiency. TPP-SD bridges the gap between powerful Transformer TPP  
13 models and the practical need for rapid sequence sampling.

## 14 1 Introduction

15 Temporal point processes (TPPs) [6] are essential stochastic models for describing discrete event  
16 occurrence patterns in continuous time. Classical models include the Poisson process [12], which  
17 is history-independent, and the Hawkes process [10], which incorporates historical dependencies.  
18 Recently, advancements in deep learning have facilitated the integration of deep models with point  
19 processes, significantly enhancing their expressive capabilities in capturing history dependence.  
20 Notable examples include models based on traditional RNNs [7], LSTMs [17], and Transformers [34,  
21 32]. RNN-type methods often suffer from vanishing or exploding gradients [24], limiting their  
22 performance. In contrast, Transformer TPPs have gained popularity for their ability to capture  
23 long-term dependencies and support parallel training.

24 Most current Transformer TPPs' research focuses on enhancing model expressiveness and training  
25 methodologies, with limited attention to improving sampling efficiency. Sampling from a learned  
26 temporal point process is essential for synthesizing event sequence data, making predictions based  
27 on observed history, validating model goodness-of-fit, and gaining insights into complex process  
28 dynamics. The standard sampling procedure employs the thinning algorithm [15, 21], which simulates  
29 events from a target process with conditional intensity  $\lambda^*(t)$  by iteratively generating candidates  $\tilde{t}_{i+1}$   
30 from a simple proposal process (e.g., homogeneous Poisson process with rate  $\bar{\lambda}$ ) and accepting with  
31 the probability  $\frac{\lambda^*(\tilde{t}_{i+1})}{\bar{\lambda}}$ , repeating until acceptance. This is highly inefficient because evaluating the  
32 acceptance probability for each proposed candidate requires a forward pass through the Transformer,  
33 potentially requiring many forward passes per single accepted event. Despite KV caching [25]  
34 reducing inference complexity from quadratic to linear, the large number of parameters in the  
35 Transformer architecture makes each forward pass computationally expensive.

Speculative decoding (SD) [5, 14] is a technique designed to accelerate token generation in large language models (LLMs). It generates multiple tokens in parallel, rather than predicting each token sequentially, thereby improving the efficiency of the sampling process. Drawing inspiration from the analogy between next-event sampling in TPPs and next-token prediction in LLMs, we investigate the potential application of SD from LLMs to Transformer TPPs, aiming to enhance sampling efficiency.

Specifically, we make the following key contributions in this work: (1) We identify a strong similarity between the thinning algorithm used in point process sampling and the SD technique in LLMs. (2) We propose TPP-SD, which successfully applies SD to Transformer TPPs, resulting in accelerated sampling. (3) Extensive experiments are conducted on both synthetic and real datasets. The results show that TPP-SD and standard autoregressive sampling produce samples from the same distribution, but TPP-SD achieves a speedup of approximately 2–6 $\times$ . Ablation studies analyze the impact of different hyperparameters.

## 2 Preliminary Knowledge

In this section, we provide background on TPPs, the thinning algorithm for TPPs, and SD for LLMs.

### 2.1 Temporal Point Processes

TPPs model discrete event sequences in continuous time, denoted as  $\mathcal{S} = \{(t_i, k_i)\}_{i=1}^N$  where  $(t_i, k_i)$  indicates an event of type  $k_i \in \mathcal{K} = \{1, \dots, K\}$  occurring at time  $t_i \in (0, T]$ , with  $0 < t_1 < \dots < t_N \leq T$  where  $N$  denotes the random number of events. TPPs can be defined using different parameterizations. One approach is to specify the conditional distribution of events. We denote  $f(t_{i+1}, k_{i+1} | \mathcal{H}_{t_i})$  to be the conditional density function (CDF) of event  $(t_{i+1}, k_{i+1})$  given the history of previous events  $(t_1, k_1), \dots, (t_i, k_i)$ . In this work,  $\mathcal{H}_{t-}$  denotes the history of events up to but excluding time  $t$ , while  $\mathcal{H}_t$  includes whether an event occurs at time  $t$ . Consequently, the joint distribution of all events can be factorized as:

$$p(\mathcal{S}) = \prod_{i=1}^N f(t_i, k_i | \mathcal{H}_{t_{i-1}}) (1 - F(T | \mathcal{H}_{t_N})),$$

where  $F(T | \mathcal{H}_{t_N}) = \int_{t_N}^T f(t | \mathcal{H}_{t_N}) dt$ ,  $f(t | \mathcal{H}_{t_i}) = \sum_{k=1}^K f(t, k | \mathcal{H}_{t_i})$ . As is customary, we further decompose  $f(t, k | \mathcal{H}_{t_i}) = f(t | \mathcal{H}_{t_i}) f(k | \mathcal{H}_{t_i}, t)$ . The term  $(1 - F(T | \mathcal{H}_{t_N}))$  is the probability that no event occurs in  $(t_N, T)$ . Another approach is to specify the conditional intensity function (CIF):

$$\lambda^*(t, k) dt dk = \frac{f(t, k | \mathcal{H}_{t_i}) dt dk}{1 - F(t | \mathcal{H}_{t_i})} = \mathbb{E}[N(dt \times dk) | \mathcal{H}_{t-}],$$

where  $*$  indicates that the CIF is dependent on the history  $\mathcal{H}_{t-}$ . These different parameterizations are equivalent because it can be easily proven that the CIF  $\lambda^*(t, k)$  and the CDF  $f(t, k | \mathcal{H}_{t_i})$  are one-to-one [33]. It is worth noting that the event timestamps can also be equivalently expressed as inter-event intervals  $\tau_i = t_i - t_{i-1}$ ,  $i = 1, \dots, N$  with  $t_0 = 0$ . Therefore, the CDF of the timestamps can also be equivalently expressed as the CDF of the inter-event intervals  $g(\tau | \mathcal{H}_{t_i}) = f(t_i + \tau | \mathcal{H}_{t_i})$ . Correspondingly, TPPs have two equivalent forms of log-likelihood expression:

$$\log p(\mathcal{S}) = \sum_{i=1}^N \log \lambda^*(t_i, k_i) - \sum_{k=1}^K \int_0^T \lambda^*(t, k) dt \quad (1)$$

$$= \sum_{i=1}^N [\log g(\tau_i | \mathcal{H}_{t_{i-1}}) + \log f(k_i | \mathcal{H}_{t_{i-1}}, t_i)] + \log(1 - G(T | \mathcal{H}_{t_N})), \quad (2)$$

where  $G(T | \mathcal{H}_{t_N}) = \int_0^{T-t_N} g(\tau | \mathcal{H}_{t_N}) d\tau$ . Eq. (1) is CIF-based, and Eq. (2) is CDF-based.

### 2.2 Thinning Algorithm for TPPs

For illustration purposes, we discuss the sequential simulation of timestamps from a point process using the thinning algorithm. Given the event history  $\mathcal{H}_{t_i}$ , to sample a timestamp from the original point process model (denoted as OriP) parameterized by CIF  $\lambda^*(t)$ , we use a proposal point process,

typically a homogeneous Poisson process (denoted as PoiP) with intensity  $\bar{\lambda} = \sup_{t \in (t_i, \infty)} \lambda^*(t)$ , to sample the next candidate timestamp:

$$\tilde{t}_{i+1} \sim \text{PoiP}(\mathcal{H}_{t_i}).$$

Next, the original point process model evaluates the candidate timestamp by calculating the conditional intensity at the given position:

$$\lambda^*(\tilde{t}_{i+1}) = \text{OriP}(\tilde{t}_{i+1}; \mathcal{H}_{t_i}).$$

Then, a rejection sampling step is applied to verify the candidate timestamp. The  $\tilde{t}_{i+1}$  is accepted if

$$\epsilon < \frac{\lambda^*(\tilde{t}_{i+1})}{\bar{\lambda}}, \quad \epsilon \sim \text{Uniform}[0, 1].$$

This rejection sampling ensures that the final sequence adheres to the original point process distribution. If the candidate timestamp is rejected, the process is repeated until a candidate is accepted. The accepted timestamp is then added to the event history, forming  $\mathcal{H}_{t_{i+1}}$ , and the procedure continues until the sequence is fully generated. The efficiency of the thinning algorithm depends heavily on the alignment between the proposal point process and the original point process. A closer alignment results in a higher acceptance rate, improving overall performance.

### 2.3 Speculative Decoding for LLMs

Autoregressive sampling in LLMs is inherently sequential and inefficient. SD addresses this inefficiency by delegating auto-regressive sampling to a smaller language model (draft model, denoted as  $\text{LLM}_{\text{dra}}$ ), which generates multiple candidate tokens sequentially given the context  $\mathbf{s}$ :

$$(c_1, q_1), \dots, (c_\gamma, q_\gamma) \sim \text{LLM}_{\text{dra}}(\mathbf{s}),$$

where  $\gamma$  is the length of candidate tokens,  $c_1, \dots, c_\gamma$  are the sampled tokens, and  $q_1, \dots, q_\gamma$  are their corresponding probability distributions. Then, the original language model (target model, denoted as  $\text{LLM}_{\text{tar}}$ ) processes these candidate tokens in parallel, producing probability distributions:

$$p_1, \dots, p_{\gamma+1} = \text{LLM}_{\text{tar}}(c_1, \dots, c_\gamma; \mathbf{s}),$$

where the extra probability distribution  $p_{\gamma+1}$  corresponds to processing the candidate token  $c_\gamma$ . A sequence of token-level rejection sampling is then applied to verify the candidate tokens. A candidate token  $c_i$  is accepted if all previous tokens are accepted and

$$\epsilon_i < \frac{p_i(c_i)}{q_i(c_i)}, \quad \epsilon_i \sim \text{Uniform}[0, 1].$$

This rejection sampling ensures that the final sequence adheres to the distribution of the target model. If  $c_i$  is the first rejected token, a replacement can be sampled from an adjusted distribution  $\text{norm}(\max(0, p_i - q_i))$ . When all candidates are accepted, an additional token is sampled from  $p_{\gamma+1}$ . The accepted tokens are then added to the context  $\mathbf{s}$ , and the process repeats until the sequence is complete. The efficiency of SD heavily depends on the alignment between the draft and target models. A closer alignment leads to a higher acceptance rate, improving overall performance.

## 3 Related Works

In this section, we discuss related works on point process sampling. In traditional statistical point processes, the CIF parameterization is generally preferred because the CDF is not a convenient way to specify history-dependent point processes. In contrast, the CIF provides a more convenient way to specify how the present depends on the past. Therefore, sampling methods in the statistical point process field are generally based on the CIF. Inverse method [26] simulates a unit-intensity Poisson process and transforms it into the desired point process using the inverse of the integrated CIF, leveraging the time-rescaling theorem [2]. However, this method is not suitable for complex processes that do not have analytical forms for the inverse of integrated CIF. Another more easily implementable sampling method is the thinning algorithm, which was originally proposed for sampling from inhomogeneous Poisson processes [15], and later adapted for history-dependent

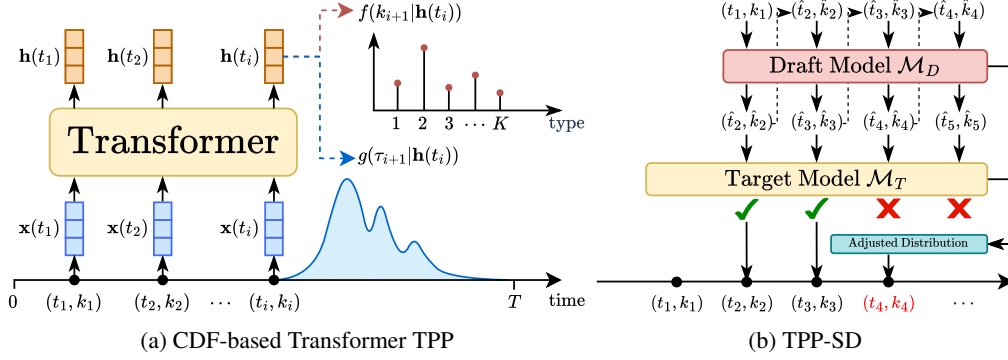


Figure 1: (a) Overall architecture of our proposed CDF-based Transformer TPP. (b) The visualization of our proposed TPP-SD sampling method as elaborated in Section 4.3.

processes [21]. With the development of the deep neural point process, an increasing number of works have started using the CDF parameterization. For example, [27] used normalizing flows and mixtures of log-normal densities to model the CDF of the inter-event interval. Although this approach was initially proposed for training convenience, another advantage it brings is facilitating sampling. This is because we can easily sample the next event directly from the CDF [22]. Whether based on CIF or CDF, both of the above methods for sampling history-dependent point processes can only be performed sequentially, leading to inefficient sampling. The key difference of this work is the introduction of parallelization in sampling, which accelerates the sampling process.

## 4 Methodology

In this section, we analyze the similarity between the thinning algorithm and the SD technique. Inspired by this insight, we propose one SD method for Transformer TPP models.

### 4.1 Thinning Algorithm v.s. Speculative Decoding

As introduced in Sections 2.2 and 2.3, the thinning algorithm and SD share significant structural similarities despite their different application domains. Both methods adopt a two-stage “propose-verify” framework that uses a draft model to generate candidates and uses the target model for verification. Besides, the efficiency of both methods critically depends on the alignment between the proposal and target distributions.

Despite these similarities, several key differences distinguish these approaches. The thinning algorithm operates strictly in an autoregressive manner, generating and verifying a single candidate timestamp per propose-verify iteration. In contrast, SD can propose and validate multiple tokens per propose-verify iteration, resulting in accelerated sampling. Additionally, while the thinning algorithm may fail to produce a valid timestamp per propose-verify iteration, SD guarantees the generation of at least one valid token per propose-verify iteration.

Motivated by these observations—especially the algorithmic similarities and the limitations of the thinning algorithm—we propose TPP-SD: a novel CDF-based sampling method for Transformer TPPs that applies the principles of SD to enhance sampling efficiency.

### 4.2 CDF-based Transformer TPPs

To accelerate TPP sampling using SD, we first need to design a CDF-based Transformer TPP model, which is composed of two parts. A similar model design has also been adopted by [22].

**Encoder.** We use Transformer backbones to model the historical dependencies in the event sequence. Specifically, given an observed realization of the point process  $\mathcal{S} = \{(t_i, k_i)\}_{i=1}^N$ , we apply the temporal encoding method from [34] to encode each timestamp  $t_i$  into a fixed-length vector  $\mathbf{z}(t_i) \in \mathbb{R}^D$ . In addition to the temporal encoding, we use an embedding matrix  $\mathbf{W} \in \mathbb{R}^{K \times D}$ , where the

144  $D$ -dimensional embedding for event type  $k_i$  is given by  $\mathbf{W}^\top \mathbf{k}_i$ , with  $\mathbf{k}_i \in \mathbb{R}^K$  being the one-hot  
 145 encoding of  $k_i$ . Thus, the embedding for the observed realization is given by

$$\mathbf{X} = f(\mathbf{KW}, \mathbf{Z}) \in \mathbb{R}^{N \times D},$$

146 where  $\mathbf{K} = [\mathbf{k}_1, \dots, \mathbf{k}_N]^\top \in \mathbb{R}^{N \times K}$  and  $\mathbf{Z} = [\mathbf{z}_1, \dots, \mathbf{z}_N]^\top \in \mathbb{R}^{N \times D}$  are the collections  
 147 of event types and timestamp embeddings of the observed realization, and  $f(\cdot, \cdot)$  is a fusion function  
 148 where we use a summation operation. A Transformer is then applied to obtain the history embedding  
 149 matrix  $\mathbf{H} = T_\theta(\mathbf{X}) \in \mathbb{R}^{N \times D}$ . Each row of the history embedding matrix  $\mathbf{h}^\top(t_i) = \mathbf{H}(i, :) \in \mathbb{R}^D$   
 150 corresponds to the history information up to timestamp  $t_i$ . The choice of encoder  $T_\theta$  can be  
 151 any Transformer TPP, such as THP [34], SAHP [32], or AttNHP [18]. The necessity of using a  
 152 Transformer encoder lies in its ability to enable parallel computation, which is essential for SD.

153 **Decoder.** Inspired by [22, 27], to enhance the flexibility of the model, we use a mixture of log-  
 154 normal distributions to model the CDF of the next timestamp  $g(\tau_{i+1}|\mathbf{h}(t_i))$ , since the inter-event  
 155 intervals are positive, i.e.,

$$g_\theta(\tau_{i+1}|\mathbf{h}(t_i)) = \sum_{m=1}^M w_{im} \frac{1}{\tau \sqrt{2\pi} \sigma_{im}} \exp\left(-\frac{(\log \tau_{i+1} - \mu_{im})^2}{2\sigma_{im}^2}\right).$$

156 Here,  $g_\theta(\tau_{i+1}|\mathbf{h}(t_i))$  is referred to as the decoder because it takes the history embedding  $\mathbf{h}(t_i)$   
 157 as input and decodes the inter-event intervals. The mixture weights  $\mathbf{w}_i = [w_{i1}, \dots, w_{iM}]^\top$ , the  
 158 mixture means  $\boldsymbol{\mu}_i = [\mu_{i1}, \dots, \mu_{iM}]^\top$ , and the mixture standard deviations  $\boldsymbol{\sigma}_i = [\sigma_{i1}, \dots, \sigma_{iM}]^\top$   
 159 are obtained by mapping  $\mathbf{h}(t_i)$ . Specifically,  $\mathbf{h}(t_i) \in \mathbb{R}^D$  is projected to  $\mathbf{e}_i = \mathbf{E}\mathbf{h}(t_i) \in \mathbb{R}^{3D}$  with  
 160  $\mathbf{E} \in \mathbb{R}^{3D \times D}$ , and then sliced into three equal-length parts  $\mathbf{e}_i = [\mathbf{e}_1^\top, \mathbf{e}_2^\top, \mathbf{e}_3^\top]^\top$ . Subsequently,  
 161  $\mathbf{e}_1^i, \mathbf{e}_2^i, \mathbf{e}_3^i$  are mapped to  $\mathbf{w}_i, \boldsymbol{\mu}_i$ , and  $\boldsymbol{\sigma}_i$  as follows:

$$\mathbf{w}_i = \text{softmax}(\mathbf{V}_w \mathbf{e}_1^i + \mathbf{b}_w), \quad \boldsymbol{\mu}_i = \mathbf{V}_\mu \mathbf{e}_2^i + \mathbf{b}_\mu, \quad \boldsymbol{\sigma}_i = \exp(\mathbf{V}_\sigma \mathbf{e}_3^i + \mathbf{b}_\sigma),$$

162 where  $\mathbf{V}_w, \mathbf{V}_\mu, \mathbf{V}_\sigma \in \mathbb{R}^{M \times D}$ , and  $\mathbf{b}_w, \mathbf{b}_\mu, \mathbf{b}_\sigma \in \mathbb{R}^M$  are learnable parameters. The CDF of the  
 163 next event type  $f_\theta(k_{i+1}|\mathbf{h}(t_i))$  is modeled as a categorical distribution:

$$f_\theta(k_{i+1}|\mathbf{h}(t_i)) = \text{softmax}\left(\mathbf{V}_k^{(2)} \tanh(\mathbf{V}_k^{(1)} \mathbf{h}(t_i) + \mathbf{b}_k^{(1)}) + \mathbf{b}_k^{(2)}\right).$$

164 Our proposed CDF-based Transformer TPP model is illustrated in Fig. 1a. This model can be formally  
 165 represented as  $\mathcal{M} = \{\mathcal{E}, g(\tau|\cdot), f(k|\cdot)\}$ , where  $\mathcal{E}$  corresponds to the encoder and  $g(\tau|\cdot), f(k|\cdot)$   
 166 correspond to the decoder. The model is trained by maximizing the log-likelihood in Eq. (2).

167 **Naïve autoregressive sampling.** The next timestamp is easy to sample from the log-normal mixture  
 168 distribution  $g_\theta(\tau_{i+1}|\mathbf{h}(t_i))$  by (see Appendix A.1 for proof)

$$\mathbf{z}_i \sim \text{Categorical}(\mathbf{w}_i), \quad \epsilon \sim \mathcal{N}(0, 1), \quad \hat{\tau}_{i+1} = \exp(\boldsymbol{\mu}_i^\top \mathbf{z}_i + \epsilon \cdot \boldsymbol{\sigma}_i^\top \mathbf{z}_i),$$

169 so the next timestamp is  $\hat{t}_{i+1} = t_i + \hat{\tau}_{i+1}$ . The next event type is sampled by  $\hat{k}_{i+1} \sim f_\theta(k_{i+1}|\mathbf{h}(t_i))$ .  
 170 The new event  $(\hat{t}_{i+1}, \hat{k}_{i+1})$  is appended to the history and the sampling procedure is repeated until we  
 171 reach the predetermined end time. However, naïve autoregressive sampling requires a forward pass  
 172 of the Transformer encoder for each event, which becomes inefficient as the number of parameters in  
 173 the Transformer backbone increases.

### 174 4.3 TPP-SD

175 Suppose we have a trained target Transformer TPP model  $\mathcal{M}_T$  with a large number of parameters,  
 176 from which we wish to sample events, and a trained draft Transformer TPP model  $\mathcal{M}_D$  with fewer  
 177 parameters, which we use to approximate  $\mathcal{M}_T$ . The procedure of TPP-SD consists of three steps, as  
 178 shown in Fig. 1b and Algorithm 1.

179 **Drafting.** Sample  $\gamma$  candidate events  $\{(\hat{t}_{i+1}, \hat{k}_{i+1}), \dots, (\hat{t}_{i+\gamma}, \hat{k}_{i+\gamma})\}$  autoregressively from  $\mathcal{M}_D$ .  
 180 Meanwhile, we record the interval CDF  $g_D(\hat{\tau}_{i+l}|\cdot)$  and type CDF  $f_D(\hat{k}_{i+l}|\cdot)$  for all candidate events.

181 **Verification.** Run  $\mathcal{M}_T$  in parallel to compute  $g_T(\hat{\tau}_{i+l}|\cdot)$  and  $f_T(\hat{k}_{i+l}|\cdot)$  for all candidate events.  
 182 Then, calculate the acceptance rates  $\frac{g_T(\hat{\tau}_{i+l}|\cdot)}{g_D(\hat{\tau}_{i+l}|\cdot)}$  and  $\frac{f_T(\hat{k}_{i+l}|\cdot)}{f_D(\hat{k}_{i+l}|\cdot)}$  for all candidate events. A candidate  
 183 inter-event interval  $\hat{\tau}_{i+l}$  is accepted if all previous events are accepted and  $\epsilon_l^\tau < \frac{g_T(\hat{\tau}_{i+l}|\cdot)}{g_D(\hat{\tau}_{i+l}|\cdot)}$ ,  $\epsilon_l^\tau \sim$   
 184 Uniform[0, 1]. A candidate event type  $\hat{k}_{i+l}$  is accepted if all previous events and  $\hat{\tau}_{i+l}$  are accepted,  
 185 and  $\epsilon_l^k < \frac{f_T(\hat{k}_{i+l}|\cdot)}{f_D(\hat{k}_{i+l}|\cdot)}$ ,  $\epsilon_l^k \sim$  Uniform[0, 1].

186 **Sampling from adjusted distribution.** Once a candidate event interval  $\hat{\tau}_{i+l}$  or type  $\hat{k}_{i+l}$  is rejected,  
 187 all subsequent candidate events are automatically discarded and a replacement  $\hat{\tau}_{i+l}$  or  $\hat{k}_{i+l}$  is sampled  
 188 from an adjusted distribution defined as below:

$$g'(\tau_{i+l}|\cdot) = \text{norm}(\max(0, g_T(\tau_{i+l}|\cdot) - g_D(\tau_{i+l}|\cdot))), \quad (3)$$

$$f'(k_{i+l}|\cdot) = \text{norm}(\max(0, f_T(k_{i+l}|\cdot) - f_D(k_{i+l}|\cdot))), \quad (4)$$

189 where  $\text{norm}(\cdot)$  denotes the normalization. The correctness and necessity of sampling from the  
 190 adjusted distribution have been established in the original speculative decoding work for LLMs [14].  
 191 In this work, we extend the proof to the TPP domain, as presented in Appendix A.2.

192 Eq. (4) is a discrete distribution, and its normalization is relatively easy to implement, but Eq. (3)  
 193 is a continuous distribution, and normalizing it is much more difficult because we need to compute  
 194 the normalizing constant  $\int \max(0, g_T(\tau_{i+l}|\cdot) - g_D(\tau_{i+l}|\cdot)) d\tau_{i+l}$ . This is also the main difference  
 195 between TPP-SD and LLM-SD, as continuous distributions are not involved in the LLM application.  
 196 Inspired by [28], we employ an acceptance-rejection sampling scheme [4] to sample from  $g'(\tau_{i+l}|\cdot)$ ,  
 197 as outlined in Theorem 1 (refer to Appendix A.3 for the proof).

198 **Theorem 1.** For a sample  $\hat{\tau}_{i+l} \sim g_T(\tau_{i+l}|\cdot)$ , define the acceptance threshold as

$$\alpha = \frac{\max(0, g_T(\hat{\tau}_{i+l}|\cdot) - g_D(\hat{\tau}_{i+l}|\cdot))}{g_T(\hat{\tau}_{i+l}|\cdot)}.$$

199 Accept  $\hat{\tau}_{i+l}$  if  $\epsilon < \alpha$ , where  $\epsilon \sim \text{Uniform}(0, 1)$ . This acceptance-rejection procedure generates  
 200 samples from the adjusted distribution  $g'(\tau_{i+l}|\cdot)$  defined in Eq. (3).

## 201 5 Experiments

202 In this section, we compare TPP-SD with autoregressive sampling (abbreviated as AR sampling)  
 203 on both synthetic and real datasets. We verify that both methods produce samples from the same  
 204 underlying distribution, and demonstrate that TPP-SD significantly improves sampling efficiency.

### 205 5.1 Evaluation of Sampling Quality and Speed

206 Unlike point process fitting, which focuses on the accuracy of predicted event types or timestamp  
 207 deviations, point process sampling emphasizes whether the samples generated by TPP-SD and AR  
 208 sampling follow the same distribution (i.e., sampling quality), as well as the efficiency of the sampling  
 209 process (i.e., sampling speed). Therefore, we define the following evaluation metrics.

210 **Likelihood Discrepancy (Synthetic and Real).** For synthetic data, where the ground truth is  
 211 known, we generate samples using both AR sampling and TPP-SD, and measure the discrepancy  
 212 between the ground-truth likelihood (Eq. (1)) and the model likelihood of the generated samples  
 213 (Eq. (2)). Specifically, we compute  $\Delta\mathcal{L}_{\text{ar}}^{\text{syn}} = |\mathcal{L}_{\text{gt}} - \mathcal{L}_{\text{ar}}|$  for AR sampling and  $\Delta\mathcal{L}_{\text{sd}}^{\text{syn}} = |\mathcal{L}_{\text{gt}} - \mathcal{L}_{\text{sd}}|$   
 214 for TPP-SD. For real data, where the ground truth is unknown, we measure the discrepancy between  
 215 the AR sampling likelihood and the TPP-SD likelihood,  $\Delta\mathcal{L}^{\text{real}} = |\mathcal{L}_{\text{ar}} - \mathcal{L}_{\text{sd}}|$ . Ideally, samples  
 216 generated by TPP-SD and AR sampling should follow the same distribution—i.e., the ground-truth  
 217 distribution. A lower likelihood discrepancy indicates higher sample quality.

218 **Kolmogorov-Smirnov Statistic (Synthetic Only).** For synthetic data where the ground truth  
 219 is known, the time-rescaling theorem [2] states that for event times  $\{t_i\}_{i=1}^n$  generated by a point  
 220 process with CIF  $\lambda^*(t)$ , if the model is correctly specified, the transformed inter-event intervals  
 221  $z_i = \int_{t_{i-1}}^{t_i} \lambda^*(\tau) d\tau$  are i.i.d. samples from Exponential(1). Therefore, we apply the ground-truth

Table 1: Performance of TPP-SD with draft length  $\gamma = 10$  against AR sampling across synthetic datasets and Transformer encoders. We conduct all experiments using three random seeds and report the mean for each metric. For all metrics, the best performance is highlighted in **bold**.

Dataset		Poisson			Hawkes			Multi-Hawkes		
Encoder Type		THP	SAHP	AttNHP	THP	SAHP	AttNHP	THP	SAHP	AttNHP
$\Delta\mathcal{L}^{\text{syn}} (\downarrow)$	AR Sampling	0.542	<b>0.012</b>	<b>1.879</b>	0.753	0.884	<b>0.220</b>	<b>0.022</b>	0.146	0.334
	TPP-SD	<b>0.349</b>	0.204	1.952	<b>0.276</b>	<b>0.630</b>	0.722	0.321	<b>0.070</b>	<b>0.199</b>
$D_{\text{KS}} (\downarrow)$	AR Sampling	0.038	<b>0.033</b>	0.076	0.044	0.031	0.029	0.069	<b>0.055</b>	0.065
	TPP-SD	<b>0.036</b>	0.050	<b>0.068</b>	<b>0.043</b>	<b>0.028</b>	<b>0.027</b>	<b>0.053</b>	0.080	<b>0.045</b>
Wall-time	AR Sampling	3.477	2.680	12.103	5.147	2.747	20.503	4.007	2.490	12.403
$T (\downarrow)$	TPP-SD	<b>1.647</b>	<b>2.077</b>	<b>4.063</b>	<b>2.547</b>	<b>1.863</b>	<b>3.567</b>	<b>1.893</b>	<b>1.647</b>	<b>2.770</b>
Speedup Ratio $S_{\text{AR/SD}} (\uparrow)$		2.110	1.290	2.967	2.113	1.513	5.743	2.117	1.277	4.467

CIF to transform the samples generated by AR sampling and TPP-SD, and then compute the KS statistic  $D_{\text{KS}}$  to assess the conformity of generated samples to the ground-truth distribution. A smaller  $D_{\text{KS}}$  indicates higher sample quality. The detailed computation of  $D_{\text{KS}}$  is provided in Appendix A.4.

**Wasserstein Distance (Real Only).** For real data where the ground truth is unknown, the KS statistic cannot be computed. Instead, we assess the sampling consistency between AR sampling and TPP-SD using the Wasserstein distance  $D_{\text{WS}}$ . Specifically, using the first  $M$  events as history, we perform  $N$  independent repetitions of sampling  $(M + 1)$ -th event, yielding  $\{(t_i^{\text{AR}}, k_i^{\text{AR}})\}_{i=1}^N$  from AR sampling and  $\{(t_i^{\text{SD}}, k_i^{\text{SD}})\}_{i=1}^N$  from TPP-SD. For the temporal distribution, we compute  $D_{\text{WS}}^t$ , the 1-Wasserstein distance between the empirical distributions of  $\{t_i^{\text{AR}}\}_{i=1}^N$  and  $\{t_i^{\text{SD}}\}_{i=1}^N$ , using `ot.wasserstein_1d` from the POT library [9]. For the event type distribution, we compute  $D_{\text{WS}}^k$ , the earth mover’s distance between the empirical distributions of  $\{k_i^{\text{AR}}\}_{i=1}^N$  and  $\{k_i^{\text{SD}}\}_{i=1}^N$ , using `ot.emd2` from the same library. A smaller  $D_{\text{WS}}$  indicates higher sample quality.

**Speedup Ratio (Synthetic and Real).** Sampling efficiency is central to this work. We quantify the acceleration gain by computing the ratio of execution wall times between AR sampling and TPP-SD, defined as  $S_{\text{AR/SD}} = \frac{T_{\text{AR}}}{T_{\text{SD}}}$ , where  $T_{\text{AR}}$  and  $T_{\text{SD}}$  denote the execution wall times of AR sampling and TPP-SD, respectively. A larger  $S_{\text{AR/SD}}$  indicates a faster sampling speed.

## 5.2 Experimental Results on Synthetic Data

**Datasets and Setup.** We consider three synthetic datasets: inhomogeneous Poisson, univariate Hawkes, and multivariate Hawkes processes, each with 1000 sequences within the time window  $[0, 100]$ . For each dataset, we train an 8-head, 20-layer target model and a 1-head, 1-layer draft model. We compare two sampling approaches: AR sampling using only the target model versus TPP-SD which combines both target and draft models as elaborated in Section 4.3. Details on data simulation procedures, data splitting, and experimental settings are provided in Appendices B.1 and C.3.1.

**Results.** As shown in Table 1, across all three synthetic datasets and three encoder architectures, TPP-SD consistently demonstrates high-fidelity sampling that closely matches the performance of AR sampling. Specifically, both TPP-SD and AR sampling exhibit low likelihood discrepancies and near-zero KS statistics relative to the ground truth, indicating excellent alignment with the target distribution. Furthermore, as shown in Fig. 2, the KS plots show that the samples generated by both methods consistently fall within the 95% confidence bands.

TPP-SD consistently achieves faster execution times and  $1.3\text{--}5.7\times$  speedup across all datasets and encoder architectures. These results demonstrate that TPP-SD maintains the same high sampling fidelity as AR sampling while providing significant improvements in sampling efficiency.

In addition, architectural variations are evident: AttNHP achieves the highest acceleration ratios despite having the slowest wall times; SAHP shows the lowest speedup but maintains the fastest wall times; and THP strikes a balance between acceleration ratio and runtime. These results suggest that the underlying architecture plays a significant role in determining the effectiveness of acceleration. A detailed discussion of these differences is provided in Appendix D.2.

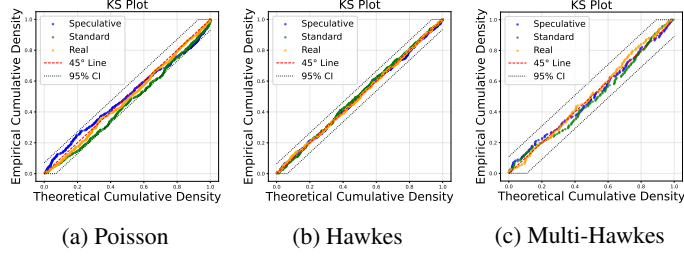


Figure 2: KS plots for (a) Poisson, (b) Hawkes, and (c) Multi-Hawkes datasets. We use AttNHP as encoder, and blue, green, and orange points represent samples from TPP-SD ( $\gamma = 10$ ), AR sampling, and ground truth, respectively. Black dotted lines show 95% KS confidence bands.

Table 2: Performance of TPP-SD with draft length  $\gamma = 10$  against AR sampling across real datasets and Transformer encoders. We conduct all experiments using three random seeds and report the mean for each metric. For all metrics, the best performance is highlighted in **bold**.

Dataset		Taobao			Amazon			Taxi			StackOverflow		
Encoder Type		THP	SAHP	AttNHP	THP	SAHP	AttNHP	THP	SAHP	AttNHP	THP	SAHP	AttNHP
$\Delta\mathcal{L}^{\text{real}} (\downarrow)$	AR Sampling	0.446	<b>0.148</b>	<b>0.629</b>	<b>0.056</b>	0.099	<b>0.118</b>	1.4411	0.563	0.859	0.587	<b>0.340</b>	0.985
	TPP-SD	<b>0.033</b>	0.746	0.860	0.129	<b>0.035</b>	0.197	<b>0.065</b>	<b>0.093</b>	<b>0.506</b>	<b>0.231</b>	0.602	<b>0.020</b>
$D_{\text{ws}}^t (\downarrow)$	AR Sampling	0.236	<b>0.328</b>	0.187	0.189	<b>0.019</b>	0.975	0.201	0.236	<b>0.249</b>	0.470	<b>0.378</b>	0.677
	TPP-SD	<b>0.076</b>	0.493	<b>0.116</b>	<b>0.078</b>	0.146	<b>0.464</b>	<b>0.082</b>	<b>0.036</b>	0.331	<b>0.391</b>	0.518	<b>0.614</b>
$D_{\text{ws}}^k (\downarrow)$	AR Sampling	<b>0.267</b>	0.414	<b>0.193</b>	<b>0.184</b>	<b>0.459</b>	<b>0.252</b>	<b>0.055</b>	0.778	<b>0.094</b>	0.376	0.381	<b>0.218</b>
	TPP-SD	0.751	<b>0.368</b>	0.206	0.418	1.409	0.327	0.655	<b>0.744</b>	0.134	<b>0.375</b>	<b>0.199</b>	0.507
Wall-time $T (\downarrow)$	AR Sampling	5.890	2.460	16.256	1.023	0.900	7.657	1.157	1.183	2.573	1.353	1.423	3.217
	TPP-SD	<b>3.460</b>	<b>1.643</b>	<b>5.180</b>	<b>0.290</b>	<b>0.317</b>	<b>1.353</b>	<b>0.453</b>	<b>0.347</b>	<b>0.650</b>	<b>0.700</b>	<b>0.663</b>	<b>0.783</b>
Speedup Ratio $S_{\text{AR/SD}} (\uparrow)$		1.597	1.553	3.183	3.550	2.847	5.849	2.553	3.637	4.310	1.930	2.153	4.290

### 5.3 Experimental Results on Real Data

**Datasets and Setup.** For real data, we consider four commonly used datasets: **Taobao** [1], **Amazon** [20], **Taxi** [29], and **StackOverflow** [8]. We similarly train an 8-head, 20-layer target model and a 1-head, 1-layer draft model as in Section 5.2, and compare the sampling performance between AR sampling and TPP-SD. Details on data statistics, data splitting, and experimental settings are provided in Appendix C.3.2. It is worth noting that for real data, the ground-truth distribution is unknown. Therefore, we use AR sampling as a reference and quantify how closely TPP-SD approximates it. To establish a meaningful baseline that accounts for the inherent stochasticity of TPP sampling, we compare two independent runs of AR sampling. In theory, the likelihood discrepancy and Wasserstein distances between two such runs should be zero. However, due to stochastic variation, even independent autoregressive runs may exhibit small differences. This self-comparison serves as a baseline for evaluating how well TPP-SD aligns with AR sampling.

**Results.** Table 2 shows TPP-SD consistently delivers high-fidelity sampling across all real datasets and encoder architectures. Similar to the observations on synthetic data,  $\Delta\mathcal{L}^{\text{real}}$  remains low, and both  $D_{\text{ws}}^t$  and  $D_{\text{ws}}^k$  approach zero, indicating strong alignment in both temporal and type distributions. Moreover, TPP-SD achieves 1.6–5.9 $\times$  faster execution across all settings. These results confirm that TPP-SD matches the sampling fidelity of AR sampling while offering substantial gains in efficiency.

An interesting observation is that the speedup inversely correlates with event type cardinality. Datasets with higher cardinality ( $K = 17$  for Taobao,  $K = 22$  for StackOverflow) tend to yield lower speedup compared to those with lower cardinality ( $K = 16$  for Amazon,  $K = 10$  for Taxi). This is because a larger number of event types increases the probability of divergence between the draft and target models, leading to more rejections during SD. Additionally, the AttNHP encoder consistently achieves greater speedups than THP and SAHP, a trend also observed in the synthetic data experiments.

### 5.4 Ablation Studies

We analyze the sensitivity of two critical hyperparameters, draft length  $\gamma$  and draft model size. Throughout this part, we adopt AttNHP encoder, and record the likelihood discrepancy  $\Delta\mathcal{L}$  ( $\Delta\mathcal{L}_{\text{sd}}^{\text{syn}}$ ).



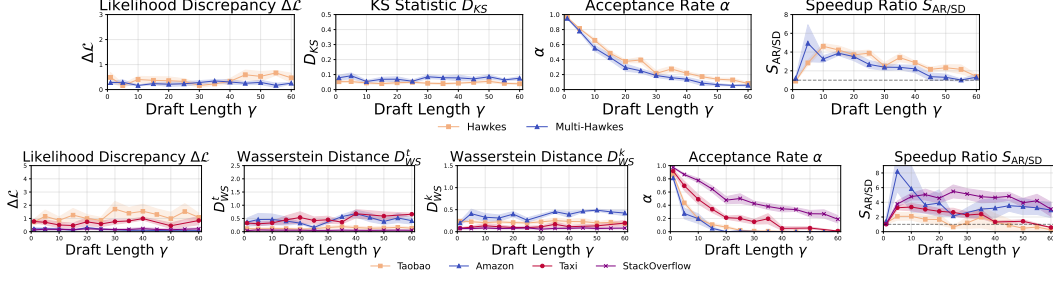


Figure 3: The impact of draft length  $\gamma$  on sampling quality measured by likelihood discrepancy ( $\Delta\mathcal{L}$ ) and distance ( $D_{KS}$  or  $D_{WS}$ ), and on sampling speed measured by speedup ratio  $S_{AR/SD}$ . We conduct all experiments using five random seeds and report the mean and the error band for each metric.

Table 3: Performance of TPP-SD with draft length  $\gamma = 10$  under different size of draft model. The distance metrics  $D_{KS}$  is used for synthetic datasets, while  $D_{WS}^t$  and  $D_{WS}^k$  are used for real datasets. We conduct all experiments using three random seeds and report the mean for each metric. For all metrics, the best performance is highlighted in **bold**, and the second best is highlighted in underline.

Dataset	Encoder Type	Draft Model head layer		$\Delta\mathcal{L}$	$D_{KS} \downarrow$	Distance $D_{WS}^t \downarrow$	$D_{WS}^k \downarrow$	$\alpha \uparrow$	Wall-time $T_{AR} \downarrow$ $T_{SD} \downarrow$		Speedup Ratio $S_{AR/SD} \uparrow$
Multi-Hawkes	AttNHP	1	1	0.098	<b>0.011</b>	-	-	0.600	12.403	<b>2.650</b>	<b>4.680</b>
		2	4	<u>0.139</u>	<u>0.009</u>	-	-	<u>0.710</u>	12.403	3.003	4.130
		4	6	<b>0.227</b>	0.004	-	-	<b>0.740</b>	12.403	5.176	2.676
Taobao	AttNHP	1	1	<u>0.276</u>	-	<b>0.080</b>	<u>0.197</u>	0.220	16.256	<b>5.727</b>	<b>2.838</b>
		2	4	<b>0.174</b>	-	<u>0.129</u>	0.200	<u>0.300</u>	16.256	<u>6.513</u>	2.496
		4	6	0.371	-	0.131	<b>0.190</b>	<b>0.35</b>	16.256	8.81	1.845

for synthetic and  $\Delta\mathcal{L}^{\text{real}}$  for real datasets), distance metrics  $D$  ( $D_{KS}$  for synthetic and  $D_{WS}$  for real datasets), acceptance rate  $\alpha = \frac{\# \text{ events accepted}}{\# \text{ events drafted}}$ , wall time  $T$  and speedup ratio  $S_{AR/SD}$ .

**Draft Length.** To identify the optimal draft length  $\gamma$  for TPP-SD, we evaluate performance across datasets within the time window  $[0, 100]$  for  $\gamma \in [1, 60]$ . Fig. 3 shows that variations in  $\gamma$  have negligible impacts on the metrics  $\Delta\mathcal{L}$  and  $D$ , confirming the distributional equivalence of TPP-SD and AR sampling. However, acceptance rate  $\alpha$  decreases as  $\gamma$  increases, and speedup  $S_{AR/SD}$  peaks before declining—falling below  $1\times$  for excessively large draft lengths due to the overhead of evaluating rejected drafts. Moderate draft lengths (e.g.,  $\gamma \approx 5\text{--}15$ ) yield the highest speedup across all datasets.

**Draft Model Size.** We investigate the impact of draft model size on performance by fixing the target model to an 8-head, 20-layer Transformer and evaluating three draft configurations: 1-head-1-layer, 2-head-4-layer, and 4-head-6-layer. Experiments are conducted on the Multi-Hawkes and Taobao datasets. Results show that increasing draft model size preserves sampling quality—as measured by  $\Delta\mathcal{L}$  and  $D$ —and improves the acceptance rate  $\alpha$ , but reduces the speedup ratio  $S_{AR/SD}$ . Notably, the 1-head-1-layer configuration achieves the highest speedup without compromising sample quality.

## 6 Conclusions

In this work, we introduce the original SD framework from the LLM domain into the context of TPP sampling. By identifying structural similarities between the thinning algorithm in TPPs and speculative decoding in LLMs, we develop an efficient framework that employs a lightweight draft model to propose candidate events for verification by the target model. TPP-SD significantly improves sampling efficiency by  $2\text{--}6\times$  while preserving distributional consistency with AR sampling, thus bridging the gap between the expressive power of Transformer TPPs and the need for efficient sequence generation in practical applications. As future work, we plan to further optimize TPP-SD by incorporating advancements in SD. Specifically, we aim to integrate the draft mechanism into the target model [3], or perform speculative decoding at the feature level rather than the event level [16].

## References

- [1] Alibaba. User behavior data from taobao for recommendation, 2018.
- [2] Emery N Brown, Riccardo Barbieri, Valérie Ventura, Robert E Kass, and Loren M Frank. The time-rescaling theorem and its application to neural spike train data analysis. *Neural computation*, 14(2):325–346, 2002.
- [3] Tianle Cai, Yuhong Li, Zhengyang Geng, Hongwu Peng, Jason D. Lee, Deming Chen, and Tri Dao. Medusa: Simple llm inference acceleration framework with multiple decoding heads. In *Proceedings of the 41st International Conference on Machine Learning, ICML’24*. JMLR.org, 2024.
- [4] George Casella, Christian P Robert, and Martin T Wells. Generalized accept-reject sampling schemes. *Lecture notes-monograph series*, pages 342–347, 2004.
- [5] Charlie Chen, Sebastian Borgeaud, Geoffrey Irving, Jean-Baptiste Lespiau, Laurent Sifre, and John Jumper. Accelerating large language model decoding with speculative sampling. *arXiv preprint arXiv:2302.01318*, 2023.
- [6] Daryl J Daley and David Vere-Jones. An introduction to the theory of point processes. vol. i. probability and its applications, 2003.
- [7] Nan Du, Hanjun Dai, Rakshit Trivedi, Utkarsh Upadhyay, Manuel Gomez-Rodriguez, and Le Song. Recurrent marked temporal point processes: embedding event history to vector. In *Proceedings of the 22nd ACM SIGKDD International Conference on Knowledge Discovery and Data Mining*, pages 1555–1564. ACM, 2016.
- [8] Nan Du, Hanjun Dai, Rakshit Trivedi, Utkarsh Upadhyay, Manuel Gomez-Rodriguez, and Le Song. Recurrent marked temporal point processes: Embedding event history to vector. In Balaji Krishnapuram, Mohak Shah, Alexander J. Smola, Charu C. Aggarwal, Dou Shen, and Rajeev Rastogi, editors, *Proceedings of the 22nd ACM SIGKDD International Conference on Knowledge Discovery and Data Mining, San Francisco, CA, USA, August 13-17, 2016*, pages 1555–1564. ACM, 2016.
- [9] Rémi Flamary, Nicolas Courty, Alexandre Gramfort, Mokhtar Z. Alaya, Aurélie Boisbunon, Stanislas Chambon, Laetitia Chapel, Adrien Corenflos, Kilian Fatras, Nemo Fournier, Léo Gautheron, Nathalie T.H. Gayraud, Hicham Janati, Alain Rakotomamonjy, Ievgen Redko, Antoine Rolet, Antony Schutz, Vivien Seguy, Danica J. Sutherland, Romain Tavenard, Alexander Tong, and Titouan Vayer. Pot: Python optimal transport. *Journal of Machine Learning Research*, 22(78):1–8, 2021.
- [10] Alan G Hawkes. Spectra of some self-exciting and mutually exciting point processes. *Biometrika*, 58(1):83–90, 1971.
- [11] Diederik P. Kingma and Jimmy Ba. Adam: A method for stochastic optimization, 2017.
- [12] John Frank Charles Kingman. *Poisson processes*, volume 3. Clarendon Press, 1992.
- [13] Donald E. Knuth. *The art of computer programming, volume 2 (3rd ed.): seminumerical algorithms*. Addison-Wesley Longman Publishing Co., Inc., USA, 1997.
- [14] Yaniv Leviathan, Matan Kalman, and Yossi Matias. Fast inference from transformers via speculative decoding. In *International Conference on Machine Learning*, pages 19274–19286. PMLR, 2023.
- [15] PA W Lewis and Gerald S Shedler. Simulation of nonhomogeneous poisson processes by thinning. *Naval research logistics quarterly*, 26(3):403–413, 1979.
- [16] Yuhui Li, Fangyun Wei, Chao Zhang, and Hongyang Zhang. Eagle: speculative sampling requires rethinking feature uncertainty. In *Proceedings of the 41st International Conference on Machine Learning, ICML’24*. JMLR.org, 2024.

- [17] Hongyuan Mei and Jason Eisner. The neural Hawkes process: A neurally self-modulating multivariate point process. In Isabelle Guyon, Ulrike von Luxburg, Samy Bengio, Hanna M. Wallach, Rob Fergus, S. V. N. Vishwanathan, and Roman Garnett, editors, *Advances in Neural Information Processing Systems 30: Annual Conference on Neural Information Processing Systems 2017, December 4-9, 2017, Long Beach, CA, USA*, pages 6754–6764, 2017.
- [18] Hongyuan Mei, Chenghao Yang, and Jason Eisner. Transformer embeddings of irregularly spaced events and their participants. In *International Conference on Learning Representations*, 2022.
- [19] Paul-André Meyer. Démonstration simplifiée d’un théorème de knight. *Séminaire de probabilités de Strasbourg*, 5:191–195, 1971.
- [20] Jianmo Ni, Jiacheng Li, and Julian McAuley. Justifying recommendations using distantly-labeled reviews and fine-grained aspects. In *Proceedings of the 2019 conference on empirical methods in natural language processing and the 9th international joint conference on natural language processing (EMNLP-IJCNLP)*, pages 188–197, 2019.
- [21] Yosihiko Ogata. On Lewis’ simulation method for point processes. *IEEE Transactions on Information Theory*, 27(1):23–31, 1981.
- [22] Aristeidis Panos. Decomposable transformer point processes. In *Annual Conference on Neural Information Processing Systems*, 2024.
- [23] F Papangelou. Integrability of expected increments of point processes and a related random change of scale. *Transactions of the American Mathematical Society*, 165:483–506, 1972.
- [24] Razvan Pascanu, Tomas Mikolov, and Yoshua Bengio. On the difficulty of training recurrent neural networks. In *Proceedings of the 30th International Conference on International Conference on Machine Learning-Volume 28*, pages III–1310, 2013.
- [25] Reiner Pope, Sholto Douglas, Aakanksha Chowdhery, Jacob Devlin, James Bradbury, Jonathan Heek, Kefan Xiao, Shivani Agrawal, and Jeff Dean. Efficiently scaling transformer inference. *Proceedings of Machine Learning and Systems*, 5:606–624, 2023.
- [26] Jakob Gulddahl Rasmussen. Lecture notes: Temporal point processes and the conditional intensity function, 2018.
- [27] Oleksandr Shchur, Marin Bilos, and Stephan Günnemann. Intensity-free learning of temporal point processes. In *8th International Conference on Learning Representations, ICLR 2020, Addis Ababa, Ethiopia, April 26-30, 2020*. OpenReview.net, 2020.
- [28] Zili Wang, Robert Zhang, Kun Ding, Qi Yang, Fei Li, and Shiming Xiang. Continuous speculative decoding for autoregressive image generation, 2024.
- [29] Chris Whong. Foiling nyc’s taxi trip data. [https://chriswhong.com/open-data/foil\\_nyc\\_taxi/](https://chriswhong.com/open-data/foil_nyc_taxi/), 2014.
- [30] Siqiao Xue, Xiaoming Shi, Zhixuan Chu, Yan Wang, Hongyan Hao, Fan Zhou, Caigao Jiang, Chen Pan, James Y. Zhang, Qingsong Wen, Jun Zhou, and Hongyuan Mei. Easytpp: Towards open benchmarking temporal point processes. In *International Conference on Learning Representations (ICLR)*, 2024.
- [31] Siqiao Xue, Xiaoming Shi, Y James Zhang, and Hongyuan Mei. Hypro: A hybridly normalized probabilistic model for long-horizon prediction of event sequences. In *Advances in Neural Information Processing Systems*, 2022.
- [32] Qiang Zhang, Aldo Lipani, Ömer Kirnap, and Emine Yilmaz. Self-attentive Hawkes process. In *Proceedings of the 37th International Conference on Machine Learning, ICML 2020, 13-18 July 2020, Virtual Event*, volume 119 of *Proceedings of Machine Learning Research*, pages 11183–11193. PMLR, 2020.
- [33] Feng Zhou, Quyu Kong, and Yixuan Zhang. Advances in temporal point processes: Bayesian, deep, and llm approaches. *arXiv preprint arXiv:2501.14291*, 2025.

- 404 [34] Simiao Zuo, Haoming Jiang, Zichong Li, Tuo Zhao, and Hongyuan Zha. Transformer Hawkes  
405 process. In *Proceedings of the 37th International Conference on Machine Learning, ICML 2020,*  
406 *13-18 July 2020, Virtual Event*, volume 119 of *Proceedings of Machine Learning Research*,  
407 pages 11692–11702. PMLR, 2020.

## A Proof of Mathematical Theorems

### A.1 Sampling from a Log-Normal Mixture Model

To sample a random variable  $\tau$  from a log-normal mixture distribution where  $w_m$  are the mixture weights,  $\mu_m$  are the location parameters and  $\sigma_m$  are the scale parameters,  $M$  is the number of mixture components

$$p(\tau) = \sum_{m=1}^M w_m \cdot \frac{1}{\tau \sqrt{2\pi\sigma_m^2}} \exp\left(-\frac{(\log \tau - \mu_m)^2}{2\sigma_m^2}\right), \quad (5)$$

we only need to do the following procedure

$$z \sim \text{Categorical}(w_1, \dots, w_M), \epsilon \in \mathcal{N}(0, 1), \tau = \exp(\mu_z + \sigma_z \cdot \epsilon), \quad (6)$$

where  $z$  is a single integer  $z \in \{1, \dots, M\}$ . By  $z \sim \text{Categorical}(w_1, \dots, w_M)$ , we choose the  $z$ -th mode of the mixture of log-normal with location and scale parameter  $(\mu_z, \sigma_z)$ . Then by using the change-of-variable formula

$$p(\tau) = p(\epsilon) \left| \frac{d\epsilon}{d\tau} \right| = \frac{1}{\sqrt{2\pi}} \cdot \exp\left(-\frac{(\log \tau - \mu_z)^2}{2\sigma_z^2}\right) \frac{1}{\sigma_z \tau} = \frac{1}{\tau \sqrt{2\pi}\sigma_z} \exp\left(-\frac{(\log \tau - \mu_z)^2}{2\sigma_z^2}\right), \quad (7)$$

which is exactly the PDF of  $\mathcal{LN}(\mu_z, \sigma_z)$ .

### A.2 Correctness of Sampling from the Adjusted Distribution

Denote  $\beta_\tau$  as the acceptance probability of candidate event interval in SD, i.e.

$$\beta_\tau = \mathbb{E}_{\tau \sim g_D(\tau_{i+l}|\cdot)} \min\left(1, \frac{g_T(\tau_{i+l}|\cdot)}{g_D(\tau_{i+l}|\cdot)}\right) = \int \min(g_T(\tau|\cdot), g_D(\tau|\cdot)) d\tau. \quad (8)$$

Note that

$$g'(\tau_{i+l}|\cdot) = \frac{\max(0, g_T(\tau_{i+l}|\cdot) - g_D(\tau_{i+l}|\cdot))}{\int \max(0, g_T(\tau_{i+l}|\cdot) - g_D(\tau_{i+l}|\cdot)) d\tau_{i+l}} = \frac{g_T(\tau_{i+l}|\cdot) - \min(g_D(\tau_{i+l}|\cdot), g_T(\tau_{i+l}|\cdot))}{1 - \beta_\tau}. \quad (9)$$

Denote  $P(\text{accept}, \tau')$  as the probability that the sample  $\tau'$  drawn by the draft model is accepted by the target model, and  $P(\text{reject}, \tau')$  as the probability that  $\tau'$  is rejected and subsequently resampled from the adjusted distribution defined in Eq. (3). By the law of total probability, the distribution of a sample  $\tau'$  drawn by SD can be calculated as

$$p(\tau') = P(\text{accept}, \tau') + P(\text{reject}, \tau') \quad (10)$$

$$= \min\left(1, \frac{g_T(\tau'|\cdot)}{g_D(\tau'|\cdot)}\right) g_D(\tau'|\cdot) + (1 - \beta_\tau) g'(\tau'|\cdot) \quad (11)$$

$$= \min\left(1, \frac{g_T(\tau'|\cdot)}{g_D(\tau'|\cdot)}\right) g_D(\tau'|\cdot) + (g_T(\tau'|\cdot) - \min(g_D(\tau'|\cdot), g_T(\tau'|\cdot))) \quad (12)$$

$$= g_T(\tau'|\cdot). \quad (13)$$

which justifies the correctness of sampling from an adjusted distribution. The derivation also shows that sampling  $\tau'$  directly from the target distribution  $g_T(\tau_{i+l}|\cdot)$  instead of the adjusted distribution  $g'(\tau_{i+l}|\cdot)$  after rejection would result in  $p(\tau') \neq g_T(\tau'|\cdot)$ , leading to incorrect sampling. Similarly, denote the acceptance probability of candidate event type in SD as  $\beta_k =$

$\mathbb{E}_{k \sim f_D(k_{i+l}|\cdot)} \min\left(1, \frac{f_T(k_{i+l}|\cdot)}{f_D(k_{i+l}|\cdot)}\right) = \sum_k \min(f_T(k|\cdot), f_D(k|\cdot))$ , we can also derive the correctness of sampling  $k' \sim f'(k_{i+l}|\cdot)$ :

$$p(k') = P(\text{accept}, k') + P(\text{reject}, k') \quad (14)$$

$$= \min\left(1, \frac{f_T(k'|\cdot)}{f_D(k'|\cdot)}\right) f_D(k'|\cdot) + (1 - \beta_k) f'(k'|\cdot) \quad (15)$$

$$= \min\left(1, \frac{f_T(k'|\cdot)}{f_D(k'|\cdot)}\right) f_D(k'|\cdot) + (f_T(k'|\cdot) - \min(f_D(k'|\cdot), f_T(k'|\cdot))) \quad (16)$$

$$= f_T(k'|\cdot). \quad (17)$$

### A.3 Proof of Theorem 1

We refer to [28] for the proof in this subsection. We begin by recalling the principle and demonstrating the correctness of the standard acceptance-rejection sampling [4], which aims to draw samples from a target distribution  $p(\tau)$  using a proposal distribution  $q(\tau)$  such that  $p(\tau) \leq Mq(\tau)$ ,  $\forall \tau \in \mathcal{T}$ , where  $\mathcal{T}$  is the support of  $p(\tau)$  and  $q(\tau)$ , and  $M \geq 1$  is a finite constant. The procedure is as follows: (1) Sample a candidate  $\hat{\tau} \sim q(\tau)$ . (2) Sample a uniform random variable  $\epsilon \sim \text{Uniform}(0, 1)$ . (3) Accept the candidate  $\hat{\tau}$  if  $\epsilon < \frac{p(\hat{\tau})}{Mq(\hat{\tau})}$ ; otherwise, reject it and return to step (1). To prove that the accepted samples follow the distribution  $p(\tau)$ , let  $\mathcal{A}$  be any measurable set within the support  $\mathcal{T}$ . The probability that an accepted sample  $\hat{\tau}$  falls into  $\mathcal{A}$  is

$$\mathbb{P}(\hat{\tau} \in \mathcal{A} | \hat{\tau} \text{ is accepted}) = \frac{\mathbb{P}(\hat{\tau} \in \mathcal{A}, \hat{\tau} \text{ is accepted})}{\mathbb{P}(\hat{\tau} \text{ is accepted})} = \frac{\mathbb{P}(\hat{\tau} \in \mathcal{A}, \hat{\tau} \text{ is accepted})}{\mathbb{P}(\hat{\tau} \in \mathcal{T}, \hat{\tau} \text{ is accepted})}. \quad (18)$$

Note that

$$\mathbb{P}(\hat{\tau} \in \mathcal{A}, \hat{\tau} \text{ is accepted}) = \int_{\mathcal{T}} \int_0^1 \mathbb{I}(\hat{\tau} \in \mathcal{A}) \mathbb{I}\left(\epsilon < \frac{p(\hat{\tau})}{Mq(\hat{\tau})}\right) p(\hat{\tau}) d\epsilon d\hat{\tau} \quad (19)$$

$$= \frac{1}{M} \int_{\mathcal{T}} \mathbb{I}(\hat{\tau} \in \mathcal{A}) \frac{p(\hat{\tau})}{q(\hat{\tau})} q(\hat{\tau}) d\hat{\tau} = \frac{1}{M} \int_{\mathcal{A}} p(\hat{\tau}) d\hat{\tau}. \quad (20)$$

Therefore,

$$\mathbb{P}(\hat{\tau} \in \mathcal{A} | \hat{\tau} \text{ is accepted}) = \frac{\int_{\mathcal{A}} p(\hat{\tau}) d\hat{\tau} / M}{\int_{\mathcal{T}} p(\hat{\tau}) d\hat{\tau} / M} = \int_{\mathcal{A}} p(\hat{\tau}) d\hat{\tau}, \quad (21)$$

which justifies the correctness of acceptance-rejection sampling. Now we apply this acceptance-rejection sampling framework to the specific scenario described in the theorem. The adjusted distribution  $g'(\tau_{i+l}|\cdot)$  defined in Eq. (3) corresponds to the target distribution  $p(\tau)$ , and  $g_T(\tau_{i+l}|\cdot)$  corresponds to the proposal distribution  $q(\tau)$ . We need to find the constant  $M$  such that for any sampled  $\hat{\tau}_{i+l}$ ,  $g'(\hat{\tau}_{i+l}|\cdot) \leq M g_T(\hat{\tau}_{i+l}|\cdot)$ . Denote  $Z = \int \max(0, g_T(\hat{\tau}_{i+l}|\cdot) - g_D(\hat{\tau}_{i+l}|\cdot)) d\hat{\tau}_{i+l}$ , note that

$$g'(\hat{\tau}_{i+l}|\cdot) = \frac{\max(0, g_T(\hat{\tau}_{i+l}|\cdot) - g_D(\hat{\tau}_{i+l}|\cdot))}{Z} \leq \frac{g_T(\hat{\tau}_{i+l}|\cdot) - g_D(\hat{\tau}_{i+l}|\cdot)}{Z} \leq \frac{g_T(\hat{\tau}_{i+l}|\cdot)}{Z}, \quad (22)$$

This inequality confirms that we can set  $M := 1/Z$  to satisfy the requirement of acceptance-rejection sampling. With  $M = \frac{1}{Z}$ , the acceptance threshold  $\alpha$  is computed as

$$\alpha = \frac{g'(\hat{\tau}_{i+l}|\cdot)}{M g_T(\hat{\tau}_{i+l}|\cdot)} = \frac{\max(0, g_T(\hat{\tau}_{i+l}|\cdot) - g_D(\hat{\tau}_{i+l}|\cdot)) / Z}{g_T(\hat{\tau}_{i+l}|\cdot) / Z} = \frac{\max(0, g_T(\hat{\tau}_{i+l}|\cdot) - g_D(\hat{\tau}_{i+l}|\cdot))}{g_T(\hat{\tau}_{i+l}|\cdot)}. \quad (23)$$

which is precisely the acceptance threshold  $\alpha$  defined in Theorem 1.

### A.4 Computation of the KS Statistic

We employ the Kolmogorov-Smirnov (KS) statistic to assess whether sampled realizations conform to ground truth distributions in synthetic point processes. For  $n$  i.i.d. ordered observations  $\{X_i\}_{i=1}^n$  from a distribution  $F(x)$ , the KS statistic is defined as  $D_{\text{KS}} = \sup_x |F_n(x) - F(x)|$ , where  $F_n(x)$  is the empirical cumulative distribution of  $\{X_i\}_{i=1}^n$ . The leverage of KS statistic is guaranteed by Theorem 2.

**Theorem 2** (Time Rescaling Theorem [19, 23]). *Given a point process with CIF  $\lambda(t|\mathcal{H}_t)$  and with occurrence times  $0 < t_1 < \dots < t_n \leq T$ , define*

$$z_1 = \int_0^{t_1} \lambda(t|\mathcal{H}_t) dt, \quad z_i = \int_{t_{i-1}}^{t_i} \lambda(t|\mathcal{H}_t) dt, \quad i = 2, \dots, n. \quad (24)$$

Then  $\{z_i\}_{i=1}^n$  are independent exponential random variables with rate parameter 1.

By transforming sampled timestamps  $\{t_i\}_{i=1}^n$  using the ground truth intensity function, we obtain rescaled intervals  $\{z_i\}_{i=1}^n$  whose empirical distribution  $F_n(x)$  should approximate  $F(x) = 1 - e^{-x}$ ,  $x > 0$  if sampling is correct. Low  $D_{\text{KS}}$  values indicate high conformity to the ground truth distribution.

## B Dataset Statistics

### B.1 Synthetic Dataset

We consider three sets of synthetic data, where each dataset contains 1000 sequences and is split into 80%/10%/10% for training/validation/testing. The data are simulated using the traditional thinning algorithm [15, 21].

**Poisson** is simulated from an inhomogeneous Poisson process with an intensity function  $\lambda(t) = A(b + \sin(\omega\pi t))$  with  $A = 5, b = 1, \omega = \frac{1}{50}$  and time span  $T = 100$ .

**Hawkes** is simulated from a single-variate Hawkes process  $\lambda(t) = \mu + \sum_{t_i < t} \alpha \exp(-\beta(t - t_i))$  with  $\mu = 2.5, \alpha = 1, \beta = 2$  and time span  $T = 100$ .

**Multi-Hawkes** is simulated from a  $M$ -dimensional Hawkes process, where the intensity for the  $j$ -th dimension is  $\lambda_j(t) = \mu_m + \sum_{i=1}^M \sum_{t_i^j < t} \alpha_{ij} \exp(-\beta_{ij}(t - t_i^j))$ . Here  $M = 2, \mu_1 = \mu_2 = 0.4, \alpha_{11} = \alpha_{22} = 1, \alpha_{12} = 0.5, \alpha_{21} = 0.1, \beta_{11} = \beta_{12} = \beta_{21} = \beta_{22} = 2$ .

### B.2 Real Dataset

We consider four sets of real data listed below. For all datasets, we maintained the standard training/validation/testing splits established in prior work.

**Taobao [1]** captures the temporal behavioral patterns of the 2,000 most engaged anonymous users on the Taobao e-commerce platform during a nine-day period from November 25th to December 3rd, 2017. The dataset encompasses  $K = 17$  distinct event categories.

**Amazon [20]** documents the chronological shopping activities of anonymous customers on the Amazon marketplace from January 2008 to October 2018. The dataset features  $K = 16$  different event categories that characterize various user interactions with the platform.

**Taxi [29]** comprises pickup and dropoff incidents for taxis operating across New York City’s five boroughs (Manhattan, Brooklyn, Queens, The Bronx, and Staten Island). Each borough-specific pickup or dropoff action is classified as a distinct event type, yielding a total of  $K = 10$  event categories.

**StackOverflow [8]** consists of sequential badge-earning events by users on the prominent question-answering platform StackOverflow. Individual users accumulate various badges over approximately a two-year timeframe, with the dataset containing  $K = 22$  unique badge types in total.

## C Additional Experiment Details

### C.1 Algorithm for TPP-SD

The pseudo code for the algorithm of TPP-SD is shown in Algorithm 1.

### C.2 Training Details

To implement our proposed CDF-based Transformer TPP model, we modified the codebase from [27]. The original RNN encoder for history aggregation was replaced with Transformer backbones proposed by THP [34], SAHP [32], and AttNHP [18]. Given that these models are CIF-based, we extracted only their Transformer architectures, utilizing implementations available in the EasyTPP [30] GitHub repository<sup>1</sup>. In line with [27], we set the history embedding dimension  $D = 64$  and the number of mixture components  $M = 64$ .

---

<sup>1</sup><https://github.com/ant-research/EasyTemporalPointProcess>

---

**Algorithm 1: TPP-SD**


---

```

1 Inputs: Initial event  $(t_0, k_0)$ , end time  $T$ , number of draft events  $\gamma$ , target model
    $\mathcal{M}_T = \{\mathcal{E}_T, g_T(\tau|\cdot), f_T(k|\cdot)\}$ , draft model  $\mathcal{M}_D = \{\mathcal{E}_D, g_D(\tau|\cdot), f_D(k|\cdot)\}$ ;
2 Initialize: Sampled events  $\mathcal{S} = \{(t_0, k_0)\}$ ,  $i \leftarrow 0$ ;
3 while  $t_i < T$  do
4   for  $l = 1$  to  $\gamma$  do
5     Sample  $\hat{\tau}_{i+l} \sim g_D(\tau|\cdot)$ , record  $g_D(\hat{\tau}_{i+l}|\cdot)$  and  $\hat{t}_{i+l} \leftarrow t_{i+l-1} + \hat{\tau}_{i+l}$ ;
6     Sample  $\hat{k}_{i+l} \sim f_D(k|\cdot)$  and record  $f_D(\hat{k}_{i+l}|\cdot)$ ;
7   Compute  $g_T(\hat{\tau}_{i+1}|\cdot), \dots, g_T(\hat{\tau}_{i+\gamma}|\cdot)$  and  $f_T(\hat{k}_{i+1}|\cdot), \dots, f_T(\hat{k}_{i+\gamma}|\cdot)$  in parallel;
8    $\epsilon_1^\tau, \dots, \epsilon_\gamma^\tau, \epsilon_1^k, \dots, \epsilon_\gamma^k \sim \text{Uniform}(0, 1)$ ;
9    $L \leftarrow \{\min(l_1, l_2) | 1 \leq l_1, l_2 \leq \gamma, \epsilon_{l_1}^\tau > \frac{g_T(\hat{\tau}_{i+l_1}|\cdot)}{g_D(\hat{\tau}_{i+l_1}|\cdot)}, \epsilon_{l_2}^k > \frac{f_T(\hat{k}_{i+l_2}|\cdot)}{f_D(\hat{k}_{i+l_2}|\cdot)}\}$ ;
10  if  $L < \gamma$  then
11    Sample  $\hat{\tau}_{i+L} \sim g'(\tau_{i+L}|\cdot)$  and  $\hat{t}_{i+L} = t_{i+L-1} + \hat{\tau}_{i+L}$ ;
12    Sample  $\hat{k}_{i+L} \sim f'(k_{i+L}|\cdot)$ ;
13     $\mathcal{S} \leftarrow \mathcal{S} \cup \{(\hat{t}_{i+1}, \hat{k}_{i+1}), \dots, (\hat{t}_{i+L}, \hat{k}_{i+L})\}$ ;
14     $i \leftarrow i + L$ ;
15     $t_i \leftarrow \hat{t}_i$ ;
16  $\mathcal{S} \leftarrow \{(t_i, k_i) | (t_i, k_i) \in \mathcal{S}, t_i \leq T\}$ ;
17 Return:  $\mathcal{S}$ 

```

---

By default, we trained an 8-head, 20-layer target model and a 1-head, 1-layer draft model for each dataset. All models were trained using the Adam optimizer [11] for up to 1000 epochs with a batch size of 16 on one single NVIDIA RTX 4090. Early stopping based on validation log-likelihood was applied to prevent overfitting.

### C.3 Sampling Details

#### C.3.1 Sampling Synthetic TPPs

For the experiments in Section 5.2, we evaluate sampling performance within the time window  $[0, 100]$ . We report the discrepancy metrics  $\Delta\mathcal{L}_{\text{ar}}^{\text{syn}}$  and  $\Delta\mathcal{L}_{\text{sd}}^{\text{syn}}$ , the KS statistics  $D_{\text{KS}}$ , the execution time  $T_{\text{AR}}$  and  $T_{\text{SD}}$ , and the resulting speedup ratio  $S_{\text{AR/SD}}$  as defined in Section 5.1. We conducted experiments across three random seeds and report the mean for each metric to ensure result robustness.

Apart from numerical metrics, we employ Kolmogorov-Smirnov plots (KS plots) to visualize sampling quality, which compare the empirical cumulative distribution  $F_n(x)$  of the rescaled intervals  $\{z_i\}_{i=1}^n$  against the theoretical cumulative distribution  $F(x) = 1 - e^{-x}$  given by [2]. The KS plot visualizes points  $\{(F(z_i), F_n(z_i))\}_{i=1}^n$ , where perfect sampling would yield points along the 45-degree line.

We conduct formal statistical assessment using the Kolmogorov-Smirnov test with the following hypotheses:

$$H_0 : F_n(x) = F(x) \quad \text{versus} \quad H_1 : F_n(x) \neq F(x), \quad (25)$$

$$\text{Reject } H_0 \text{ if: } D_{\text{KS}} > \frac{c(\alpha)}{\sqrt{n}}, \quad (26)$$

where  $n$  is the number of sampled events,  $D_{\text{KS}} = \sup_x |F_n(x) - F(x)|$  is the KS statistic, and  $c(\alpha) = 1.36$  at significance level  $\alpha = 0.05$  [13]. Based on this test, we construct a 95% confidence band  $CB = \{(F(x), y) : y \in [F(x) - \frac{c(\alpha)}{\sqrt{n}}, F(x) + \frac{c(\alpha)}{\sqrt{n}}]\}$  for each KS plot. If the sampled events conform to the ground truth process at the 95% confidence level, all points in the KS plot should fall within this band.

We construct direct comparison visualizations between  $F_n(x)$  and  $F(x) = 1 - e^{-x}$  alongside KS plots across Transformer encoders (THP, SAHP, AttNHP) with draft length  $\gamma = 10$  on three synthetic datasets. As evidenced in Fig. 4,  $F_n(x)$  demonstrates strong concordance with  $F(x) = 1 - e^{-x}$ , and all points in the KS plots remain within the 95% confidence bands, providing robust statistical evidence for the distributional fidelity of our TPP-SD method.



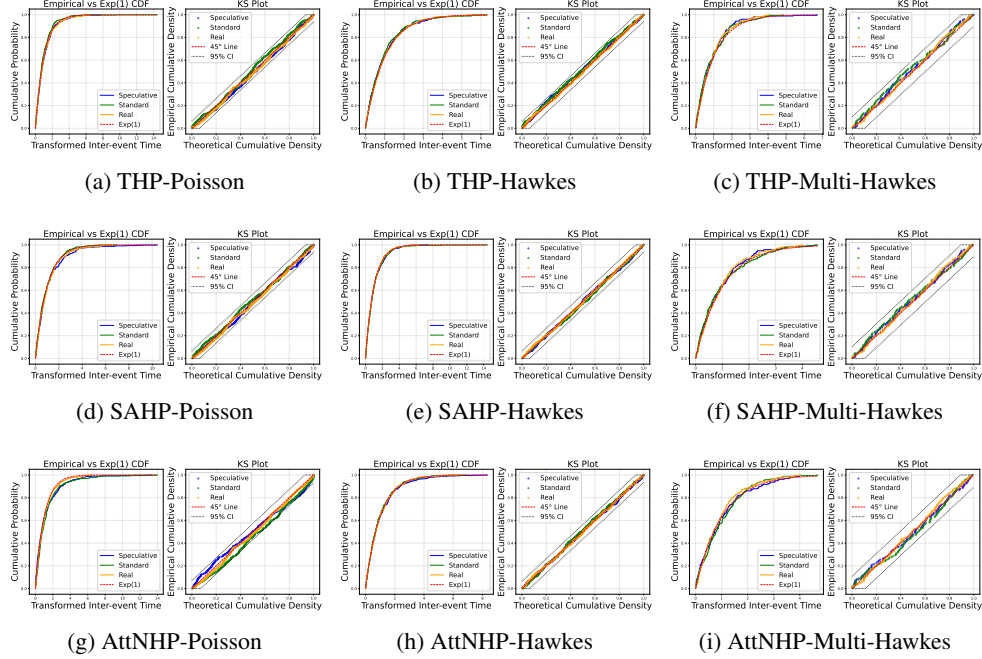


Figure 4: KS plots across THP (top row), SAHP (middle row), and AttNHP (bottom row) encoders with draft length  $\gamma = 10$  on three synthetic datasets: Poisson (left column), Hawkes (middle column), and Multi-Hawkes (right column). Blue, green, and orange points represent samples from TPP-SD ( $\gamma = 10$ ), AR sampling, and ground truth, respectively. Black dotted lines show 95% KS confidence bands.

### 528 C.3.2 Sampling Real-world TPPs

529 For the experiments in Section 5.3, we conduct evaluations within the same time window of  $[0, 100]$ .  
 530 In accordance with Appendix C.3.1, we report the discrepancy metric  $\Delta\mathcal{L}^{\text{real}}$ , the Wasserstein  
 531 distance  $D_{\text{WS}}^t$  and  $D_{\text{WS}}^k$ , the execution time  $T_{\text{AR}}$  and  $T_{\text{SD}}$  for AR sampling and TPP-SD, and the  
 532 resulting speedup ratio  $S_{\text{AR/SD}}$  defined in Section 5.1. For computation of  $D_{\text{WS}}^t$  and  $D_{\text{WS}}^k$ , we set  
 533  $M = 100$ ,  $N = 100$ , which means that we fix the first  $M = 100$  events as history and perform  
 534  $N = 100$  independent repetitions of sampling the 101-th event, obtaining  $\{(t_i^{\text{AR}}, k_i^{\text{AR}})\}_{i=1}^{100}$  from  
 535 AR sampling and  $\{(t_i^{\text{SD}}, k_i^{\text{SD}})\}_{i=1}^{100}$  from TPP-SD, and subsequently computing  $D_{\text{WS}}^t$  and  $D_{\text{WS}}^k$  as  
 536 elaborated in Section 5.1.

537 Beyond numerical metrics, we visualize event type distributions to qualitatively assess the sam-  
 538 pling fidelity of TPP-SD on real datasets, where accurate event type sampling is critical. Figure 5  
 539 demonstrates that event type distributions from TPP-SD ( $\{k_i^{\text{SD}}\}$ ) consistently align with those from  
 540 AR sampling ( $\{k_i^{\text{AR}}\}$ ) across all datasets and encoder architectures, confirming TPP-SD’s ability to  
 541 maintain distributional consistency with AR sampling in event type generation.

### 542 C.4 Ablation Studies

543 We have investigated the impact of draft length  $\gamma$  and draft model size on the sampling quality  
 544 and sampling speed of TPP-SD with AttNHP encoder. Using the same sampling configuration and  
 545 evaluation metrics as in Section 5.4, we also conducted experiments using THP and SAHP encoders.

546 **Draft Length.** As illustrated in Figs. 6a and 6b, experiments with THP and SAHP encoders reveal  
 547 patterns consistent with our findings in Section 5.4: changes in draft length  $\gamma$  minimally affect  
 548 likelihood discrepancy  $\Delta\mathcal{L}$  and distance metrics  $D$ , while acceptance rate  $\alpha$  also diminishes with  
 549 increasing  $\gamma$ , and speedup ratio  $S_{\text{AR/SD}}$  exhibits a characteristic peak followed by a decline, eventually  
 550 dropping below  $1\times$  when draft lengths become excessive. Intermediate draft lengths ( $\gamma \approx 5\text{--}15$ )  
 551 optimize computational efficiency across all experimental configurations.

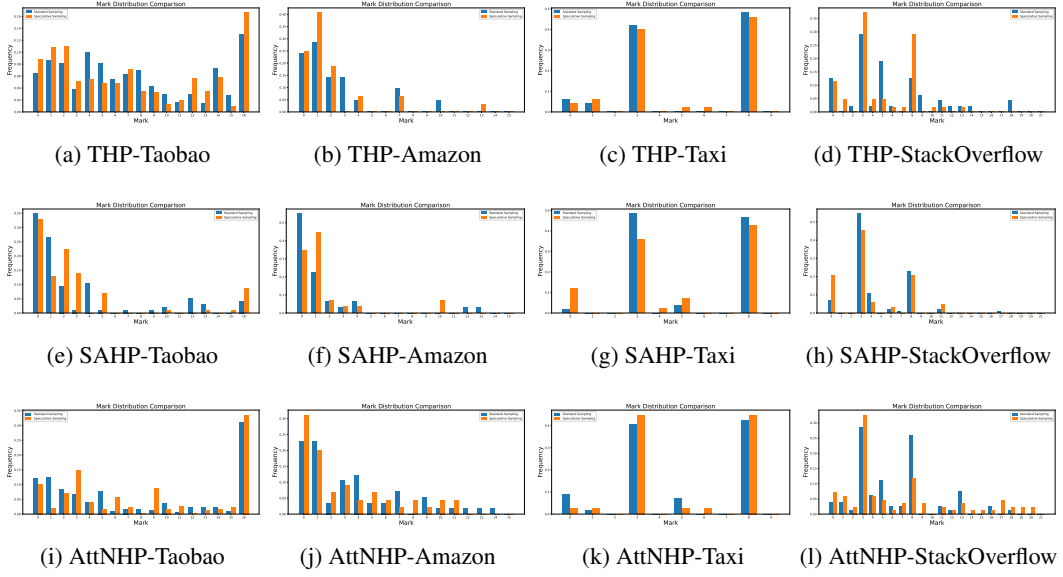


Figure 5: Event type histogram across THP (top row), SAHP (middle row), and AttNHP (bottom row) encoders with draft length  $\gamma = 10$  on four real datasets: Taobao, Amazon, Taxi and StackOverflow. Blue bars and orange bars represent the frequency of sampled event types from AR sampling and TPP-SD.

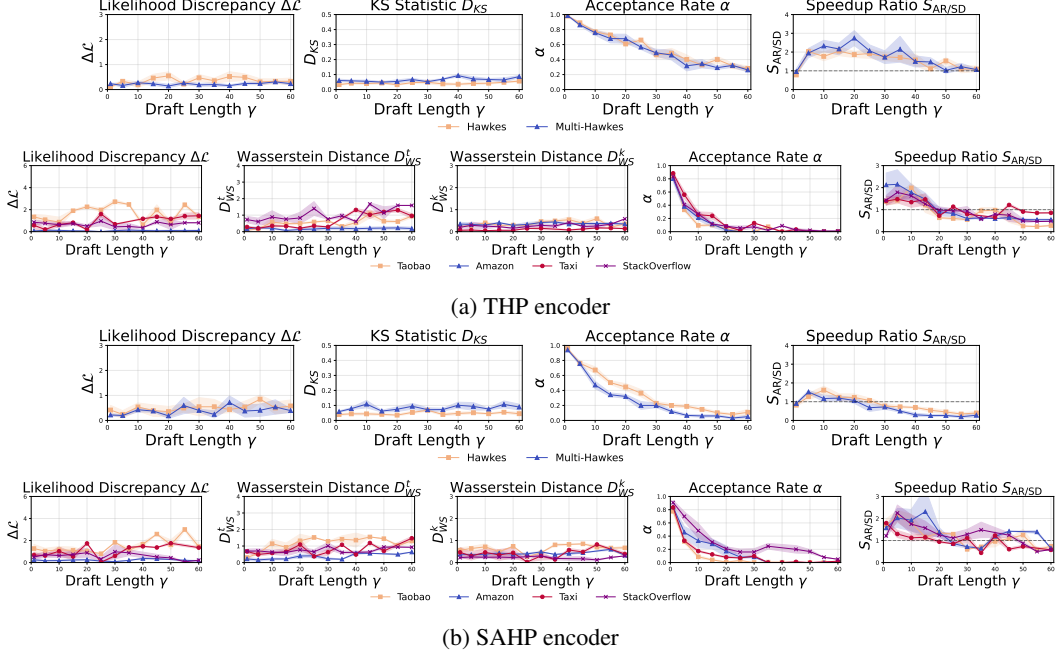


Figure 6: The impact of draft length on sampling quality measured by likelihood discrepancy ( $\Delta\mathcal{L}$ ) and distance ( $D_{KS}$  or  $D_{WS}$ ), and on sampling speed measured up speedup ratio  $S_{AR/SD}$ . We conduct experiments across five random seeds with (a) THP encoder and (b) SAHP encoder, and report the average for each metric.

**Draft Model Size.** As evidenced by Table 4, increasing the draft model size with either THP or SAHP encoder preserves sampling quality (measured by  $\Delta\mathcal{L}$  and  $D$ ) and improves the acceptance rate  $\alpha$ , but reduces the speedup ratio  $S_{AR/SD}$ . The 1-head, 1-layer configuration remains optimal for the draft model across these encoder architectures.

Table 4: Performance of TPP-SD with draft length  $\gamma = 10$  under different size of draft model. The distance metrics include KS statistic ( $D_{KS}$ ) for synthetic datasets and Wasserstein Distance ( $D_{WS}^t$ ,  $D_{WS}^k$ ) for real datasets. We conducted experiments across three random seeds and report the mean for each metric. For all metrics, the best result is shown in **bold**, and the second best result is shown in underline.

Dataset	Encoder Type	Draft Model		$\Delta\mathcal{L}$	Distance			$\alpha$ ( $\uparrow$ )	Wall-time		Speedup Ratio $S_{AR/SD}$ ( $\uparrow$ )
		head	layer		$D_{KS}$ ( $\downarrow$ )	$D_{WS}^t$ ( $\downarrow$ )	$D_{WS}^k$ ( $\downarrow$ )		$T_{AR}$ ( $\downarrow$ )	$T_{SD}$ ( $\downarrow$ )	
Multi-Hawkes	THP	1	1	0.226	<u>0.008</u>	-	-	0.790	3.990	<b>1.970</b>	<b>2.025</b>
		2	4	<u>0.202</u>	0.019	-	-	<u>0.830</u>	3.990	<u>2.179</u>	<u>1.831</u>
		4	6	<b>0.144</b>	<b>0.006</b>	-	-	<b>0.950</b>	3.990	2.208	1.807
Multi-Hawkes	SAHP	1	1	<b>0.054</b>	<u>0.008</u>	-	-	0.640	3.543	<b>2.143</b>	<b>1.653</b>
		2	4	<u>0.143</u>	<b>0.004</b>	-	-	<u>0.740</u>	3.543	<u>2.669</u>	<u>1.327</u>
		4	6	0.395	<u>0.008</u>	-	-	<b>0.800</b>	3.543	2.734	1.296
Taobao	THP	1	1	<b>0.033</b>	-	<b>0.175</b>	<b>0.222</b>	0.18	5.890	<b>3.460</b>	<b>1.702</b>
		2	4	<u>0.307</u>	-	<b>0.175</b>	0.339	<u>0.210</u>	5.890	<u>3.900</u>	<u>1.510</u>
		4	6	0.409	-	<u>0.291</u>	<u>0.301</u>	<b>0.240</b>	5.890	4.920	1.197
Taobao	SAHP	1	1	<u>0.410</u>	-	<b>0.302</b>	<b>0.630</b>	<b>0.14</b>	2.460	<b>1.621</b>	<b>1.518</b>
		2	4	<b>0.334</b>	-	<u>0.403</u>	<u>0.742</u>	<u>0.19</u>	2.460	<u>1.850</u>	<u>1.330</u>
		4	6	0.486	-	0.545	0.745	0.21	2.460	1.990	1.236

## D Additional Discussions

### D.1 Why Not Use CIF-based Speculative Decoding?

In theory, CIF-based speculative decoding is feasible. For example, we can use a homogeneous Poisson process with constant intensity  $\bar{\lambda}$  as the draft model to generate candidate timestamps  $\{\tilde{t}_i\}$ . These candidates are then input into a CIF-based Transformer point process to compute the CIF at each position,  $\{\lambda^*(\tilde{t}_i)\}$ , and the acceptance ratio  $\{\lambda^*(\tilde{t}_i)/\bar{\lambda}\}$ . A candidate timestamp  $t_i$  is accepted if all previous timestamps are accepted and  $\epsilon < \frac{\lambda^*(\tilde{t}_i)}{\bar{\lambda}}$ , where  $\epsilon \sim \text{Uniform}[0, 1]$ . However, it has two significant drawbacks: (1) Determining  $\bar{\lambda}$  is challenging because we must ensure that  $\bar{\lambda}$  is greater than the CIF at all candidate timestamps, and the CIF values are history-dependent and stochastic. To be safe, we generally have to use a relatively large  $\bar{\lambda}$ , which reduces the acceptance rate and leads to low sampling efficiency. (2) The CIF-based TPP-SD may fail to generate any valid timestamp in each iteration. If the first proposed timestamp is rejected, the CDF-based TPP-SD can sample a replacement from  $g_T(\tau|\cdot)$ , but the CIF-based method cannot do this. This can result in cases where a single forward pass of the target model fails to generate any valid timestamp, further reducing sampling efficiency.

### D.2 Architectural Differences across Encoders

We incorporate the history encoders from THP, SAHP, and AttNHP into our CDF-based Transformer TPPs designed for TPP-SD. The architectural and implementation differences among these encoders may explain the varying sampling speed performance observed in Table 1 and Table 2.

Following the notation in Section 4.2, the temporal encoding  $\mathbf{z}(t_i) \in \mathbb{R}^D$  for each encoder differs slightly:

$$\text{THP: } [\mathbf{z}(t_i)]_j = \begin{cases} \sin(t_i/10000^{j/D}) & j \text{ is even} \\ \cos(t_i/10000^{(j-1)/D}) & j \text{ is odd} \end{cases}, \quad (27)$$

$$\text{SAHP: } [\mathbf{z}(t_i)]_j = \begin{cases} \sin(j/10000^{j/D} + w_j t_i) & j \text{ is even} \\ \cos(j/10000^{(j-1)/D} + w_j t_i) & j \text{ is odd} \end{cases}, \quad (28)$$

$$\text{AttNHP: } [\mathbf{z}(t_i)]_j = \begin{cases} \sin(t_i/m \cdot (5M/m)^{j/D}) & j \text{ is even} \\ \sin(t_i/m \cdot (5M/m)^{(j-1)/D}) & j \text{ is odd} \end{cases}, \quad (29)$$

where  $[\mathbf{z}(t_i)]_j$  is the  $j$ -th dimension of the temporal embedding vector  $\mathbf{z}(t_i)$ , and  $M, m$  are hyperparameters in AttNHP.

The attention mechanisms differ across encoder architectures. For clarity, we present the single-head attention formulation for each model. The layer- $l$  history embedding of event  $(t_i, k_i)$  is computed as:

$$\text{THP/SAHP: } \mathbf{h}^{(l)}(t_i) = \mathbf{h}^{(l-1)}(t_i) + \sum_{j=1}^i \frac{f(\mathbf{q}^{(l)}(t_j), \mathbf{k}^{(l)}(t_i)) \mathbf{v}^{(l)}(t_j)}{\sum_{j=1}^i f(\mathbf{q}^{(l)}(t_j), \mathbf{k}^{(l)}(t_i))}, \quad (30)$$

$$\text{AttNHP: } \mathbf{h}^{(l)}(t_i) = \mathbf{h}^{(l-1)}(t_i) + \tanh \left( \sum_{j=1}^i \frac{f(\mathbf{q}^{(l)}(t_j), \mathbf{k}^{(l)}(t_i)) \mathbf{v}^{(l)}(t_j)}{1 + \sum_{j=1}^i f(\mathbf{q}^{(l)}(t_j), \mathbf{k}^{(l)}(t_i))} \right), \quad (31)$$

where  $f(\cdot, \cdot)$  is a Gaussian kernel  $f(\mathbf{q}^{(l)}(t_j), \mathbf{k}^{(l)}(t_i)) = \exp(-\frac{1}{\sqrt{D}} \mathbf{q}^{(l)}(t_j)^\top \mathbf{k}^{(l)}(t_i)) \in \mathbb{R}$ . The key distinction lies in how query, key, and value vectors are derived at layer- $l$ . In THP and SAHP,  $\mathbf{q}^{(l)}(t_i) = \mathbf{Q}^{(l)} \mathbf{h}^{(l-1)}$ ,  $\mathbf{k}^{(l)}(t_i) = \mathbf{K}^{(l)} \mathbf{h}^{(l-1)}$ ,  $\mathbf{v}^{(l)}(t_i) = \mathbf{V}^{(l)} \mathbf{h}^{(l-1)}$  are obtained through linear projection, whereas in AttNHP:

$$\mathbf{q}^{(l-1)}(t_i) = \mathbf{Q}^{(l)} \text{concat}(1; \mathbf{z}(t_i)^\top; \mathbf{h}^{(l-1)}(t_i)^\top)^\top, \quad (32)$$

$$\mathbf{k}^{(l-1)}(t_i) = \mathbf{K}^{(l)} \text{concat}(1; \mathbf{z}(t_i)^\top; \mathbf{h}^{(l-1)}(t_i)^\top)^\top, \quad (33)$$

$$\mathbf{v}^{(l-1)}(t_i) = \mathbf{V}^{(l)} \text{concat}(1; \mathbf{z}(t_i)^\top; \mathbf{h}^{(l-1)}(t_i)^\top)^\top, \quad (34)$$

where  $\mathbf{Q}^{(l)}, \mathbf{K}^{(l)}, \mathbf{V}^{(l)} \in \mathbb{R}^{D \times (2D+1)}$ . AttNHP's complex attention mechanism doubles the dimension of intermediate vectors, particularly in multi-head configurations where each head requires separate query, key, and value transformations. This architectural complexity results in significantly higher AR sampling latency compared to other models, making AttNHP an ideal candidate for acceleration via TPP-SD, where it achieves the largest speedup. Despite architectural similarities between THP and SAHP, implementation differences result in SAHP consistently achieving the shortest wall-time for both AR sampling and TPP-SD, leaving less room for additional acceleration.

### D.3 Differences between TPP Sampling and Long-horizon Prediction

While both TPP sampling and long-horizon prediction [31, 22] involve generating sequences of events over a continuous time interval given some history, they have fundamental differences. TPP sampling focuses on generating events from the correct distribution. Since sampling is inherently stochastic, comparing the exact events sampled with specific test set events isn't meaningful - the same distribution that we sample from can produce different event in each iteration. What matters is whether the sampled sequences follow the correct statistical patterns. On synthetic datasets, we evaluate the distributional conformity of sampled sequences from TPP-SD to the ground truth using [2] and KS statistic. On real datasets, we measure the distributional discrepancy between the sampled sequences from autoregressive sampling and TPP-SD with Wasserstein distance.

In contrast, long-horizon prediction specifically aims to forecast future events that closely match the ground truth on the test set. It's evaluated by metrics such as RMSE and optimal transport distance (OTD) that directly measure the discrepancy between predicted sequences and test-set sequences.

### D.4 Limitations

Compared to the thinning algorithm, our proposed TPP-SD is deep-learning based which requires large amount of event sequence data to learn the model's parameters. Therefore, the model is less suitable for sampling in data-scarce scenarios.

Besides, TPP-SD adopts the original SD framework from the LLM domain and requires deploying two models at the same time for accelerating sampling, which is slightly more computational demanding and less convenient. Recent advances in SD techniques [3, 16] can be incorporated to further optimize TPP-SD, and we leave this as future work.

## NeurIPS Paper Checklist

### 1. Claims

Question: Do the main claims made in the abstract and introduction accurately reflect the paper's contributions and scope?

Answer: [\[Yes\]](#)

Justification: The main claims made in the abstract and introduction accurately reflect the paper's contributions and scope. See the Abstract and Introduction sections.

Guidelines:

- The answer NA means that the abstract and introduction do not include the claims made in the paper.
- The abstract and/or introduction should clearly state the claims made, including the contributions made in the paper and important assumptions and limitations. A No or NA answer to this question will not be perceived well by the reviewers.
- The claims made should match theoretical and experimental results, and reflect how much the results can be expected to generalize to other settings.
- It is fine to include aspirational goals as motivation as long as it is clear that these goals are not attained by the paper.

### 2. Limitations

Question: Does the paper discuss the limitations of the work performed by the authors?

Answer: [\[Yes\]](#)

Justification: The limitation of the work is discussed in the appendix.

Guidelines:

- The answer NA means that the paper has no limitation while the answer No means that the paper has limitations, but those are not discussed in the paper.
- The authors are encouraged to create a separate "Limitations" section in their paper.
- The paper should point out any strong assumptions and how robust the results are to violations of these assumptions (e.g., independence assumptions, noiseless settings, model well-specification, asymptotic approximations only holding locally). The authors should reflect on how these assumptions might be violated in practice and what the implications would be.
- The authors should reflect on the scope of the claims made, e.g., if the approach was only tested on a few datasets or with a few runs. In general, empirical results often depend on implicit assumptions, which should be articulated.
- The authors should reflect on the factors that influence the performance of the approach. For example, a facial recognition algorithm may perform poorly when image resolution is low or images are taken in low lighting. Or a speech-to-text system might not be used reliably to provide closed captions for online lectures because it fails to handle technical jargon.
- The authors should discuss the computational efficiency of the proposed algorithms and how they scale with dataset size.
- If applicable, the authors should discuss possible limitations of their approach to address problems of privacy and fairness.
- While the authors might fear that complete honesty about limitations might be used by reviewers as grounds for rejection, a worse outcome might be that reviewers discover limitations that aren't acknowledged in the paper. The authors should use their best judgment and recognize that individual actions in favor of transparency play an important role in developing norms that preserve the integrity of the community. Reviewers will be specifically instructed to not penalize honesty concerning limitations.

### 3. Theory assumptions and proofs

Question: For each theoretical result, does the paper provide the full set of assumptions and a complete (and correct) proof?

Answer: [\[Yes\]](#)

Justification: For all theoretical results, the paper provides the corresponding proofs in the appendix.

Guidelines:

- The answer NA means that the paper does not include theoretical results.
- All the theorems, formulas, and proofs in the paper should be numbered and cross-referenced.
- All assumptions should be clearly stated or referenced in the statement of any theorems.
- The proofs can either appear in the main paper or the supplemental material, but if they appear in the supplemental material, the authors are encouraged to provide a short proof sketch to provide intuition.
- Inversely, any informal proof provided in the core of the paper should be complemented by formal proofs provided in appendix or supplemental material.
- Theorems and Lemmas that the proof relies upon should be properly referenced.

#### 4. Experimental result reproducibility

Question: Does the paper fully disclose all the information needed to reproduce the main experimental results of the paper to the extent that it affects the main claims and/or conclusions of the paper (regardless of whether the code and data are provided or not)?

Answer: [\[Yes\]](#)

Justification: The paper fully discloses all the information needed to reproduce the main experimental results in the paper. See the Experiments section.

Guidelines:

- The answer NA means that the paper does not include experiments.
- If the paper includes experiments, a No answer to this question will not be perceived well by the reviewers: Making the paper reproducible is important, regardless of whether the code and data are provided or not.
- If the contribution is a dataset and/or model, the authors should describe the steps taken to make their results reproducible or verifiable.
- Depending on the contribution, reproducibility can be accomplished in various ways. For example, if the contribution is a novel architecture, describing the architecture fully might suffice, or if the contribution is a specific model and empirical evaluation, it may be necessary to either make it possible for others to replicate the model with the same dataset, or provide access to the model. In general, releasing code and data is often one good way to accomplish this, but reproducibility can also be provided via detailed instructions for how to replicate the results, access to a hosted model (e.g., in the case of a large language model), releasing of a model checkpoint, or other means that are appropriate to the research performed.
- While NeurIPS does not require releasing code, the conference does require all submissions to provide some reasonable avenue for reproducibility, which may depend on the nature of the contribution. For example
  - (a) If the contribution is primarily a new algorithm, the paper should make it clear how to reproduce that algorithm.
  - (b) If the contribution is primarily a new model architecture, the paper should describe the architecture clearly and fully.
  - (c) If the contribution is a new model (e.g., a large language model), then there should either be a way to access this model for reproducing the results or a way to reproduce the model (e.g., with an open-source dataset or instructions for how to construct the dataset).
  - (d) We recognize that reproducibility may be tricky in some cases, in which case authors are welcome to describe the particular way they provide for reproducibility. In the case of closed-source models, it may be that access to the model is limited in some way (e.g., to registered users), but it should be possible for other researchers to have some path to reproducing or verifying the results.

#### 5. Open access to data and code

Question: Does the paper provide open access to the data and code, with sufficient instructions to faithfully reproduce the main experimental results, as described in supplemental material?

Answer: [Yes]

Justification: We provide the data and code in the supplemental material to reproduce the main experimental results.

Guidelines:

- The answer NA means that paper does not include experiments requiring code.
- Please see the NeurIPS code and data submission guidelines (<https://nips.cc/public/guides/CodeSubmissionPolicy>) for more details.
- While we encourage the release of code and data, we understand that this might not be possible, so “No” is an acceptable answer. Papers cannot be rejected simply for not including code, unless this is central to the contribution (e.g., for a new open-source benchmark).
- The instructions should contain the exact command and environment needed to run to reproduce the results. See the NeurIPS code and data submission guidelines (<https://nips.cc/public/guides/CodeSubmissionPolicy>) for more details.
- The authors should provide instructions on data access and preparation, including how to access the raw data, preprocessed data, intermediate data, and generated data, etc.
- The authors should provide scripts to reproduce all experimental results for the new proposed method and baselines. If only a subset of experiments are reproducible, they should state which ones are omitted from the script and why.
- At submission time, to preserve anonymity, the authors should release anonymized versions (if applicable).
- Providing as much information as possible in supplemental material (appended to the paper) is recommended, but including URLs to data and code is permitted.

## 6. Experimental setting/details

Question: Does the paper specify all the training and test details (e.g., data splits, hyperparameters, how they were chosen, type of optimizer, etc.) necessary to understand the results?

Answer: [Yes]

Justification: We specify all the training and test details necessary to understand the results. See the Experiments section.

Guidelines:

- The answer NA means that the paper does not include experiments.
- The experimental setting should be presented in the core of the paper to a level of detail that is necessary to appreciate the results and make sense of them.
- The full details can be provided either with the code, in appendix, or as supplemental material.

## 7. Experiment statistical significance

Question: Does the paper report error bars suitably and correctly defined or other appropriate information about the statistical significance of the experiments?

Answer: [Yes]

Justification: We report the statistical significance of the experiments. In the figures presenting the experimental results, we provide the standard deviations across multiple runs.

Guidelines:

- The answer NA means that the paper does not include experiments.
- The authors should answer "Yes" if the results are accompanied by error bars, confidence intervals, or statistical significance tests, at least for the experiments that support the main claims of the paper.

- The factors of variability that the error bars are capturing should be clearly stated (for example, train/test split, initialization, random drawing of some parameter, or overall run with given experimental conditions).
- The method for calculating the error bars should be explained (closed form formula, call to a library function, bootstrap, etc.)
- The assumptions made should be given (e.g., Normally distributed errors).
- It should be clear whether the error bar is the standard deviation or the standard error of the mean.
- It is OK to report 1-sigma error bars, but one should state it. The authors should preferably report a 2-sigma error bar than state that they have a 96% CI, if the hypothesis of Normality of errors is not verified.
- For asymmetric distributions, the authors should be careful not to show in tables or figures symmetric error bars that would yield results that are out of range (e.g. negative error rates).
- If error bars are reported in tables or plots, The authors should explain in the text how they were calculated and reference the corresponding figures or tables in the text.

## 8. Experiments compute resources

Question: For each experiment, does the paper provide sufficient information on the computer resources (type of compute workers, memory, time of execution) needed to reproduce the experiments?

Answer: [Yes]

Justification: All experiments are conducted on the server whose details are provided in the paper. See the Experiments section.

Guidelines:

- The answer NA means that the paper does not include experiments.
- The paper should indicate the type of compute workers CPU or GPU, internal cluster, or cloud provider, including relevant memory and storage.
- The paper should provide the amount of compute required for each of the individual experimental runs as well as estimate the total compute.
- The paper should disclose whether the full research project required more compute than the experiments reported in the paper (e.g., preliminary or failed experiments that didn't make it into the paper).

## 9. Code of ethics

Question: Does the research conducted in the paper conform, in every respect, with the NeurIPS Code of Ethics <https://neurips.cc/public/EthicsGuidelines>?

Answer: [Yes]

Justification: The research conducted in the paper conform with the NeurIPS Code of Ethics.

Guidelines:

- The answer NA means that the authors have not reviewed the NeurIPS Code of Ethics.
- If the authors answer No, they should explain the special circumstances that require a deviation from the Code of Ethics.
- The authors should make sure to preserve anonymity (e.g., if there is a special consideration due to laws or regulations in their jurisdiction).

## 10. Broader impacts

Question: Does the paper discuss both potential positive societal impacts and negative societal impacts of the work performed?

Answer: [No]

Justification: This paper presents work whose goal is to advance the field of machine learning. There are many potential societal consequences of our work, none of which we feel must be specifically highlighted here.

Guidelines:



- The answer NA means that there is no societal impact of the work performed.
- If the authors answer NA or No, they should explain why their work has no societal impact or why the paper does not address societal impact.
- Examples of negative societal impacts include potential malicious or unintended uses (e.g., disinformation, generating fake profiles, surveillance), fairness considerations (e.g., deployment of technologies that could make decisions that unfairly impact specific groups), privacy considerations, and security considerations.
- The conference expects that many papers will be foundational research and not tied to particular applications, let alone deployments. However, if there is a direct path to any negative applications, the authors should point it out. For example, it is legitimate to point out that an improvement in the quality of generative models could be used to generate deepfakes for disinformation. On the other hand, it is not needed to point out that a generic algorithm for optimizing neural networks could enable people to train models that generate Deepfakes faster.
- The authors should consider possible harms that could arise when the technology is being used as intended and functioning correctly, harms that could arise when the technology is being used as intended but gives incorrect results, and harms following from (intentional or unintentional) misuse of the technology.
- If there are negative societal impacts, the authors could also discuss possible mitigation strategies (e.g., gated release of models, providing defenses in addition to attacks, mechanisms for monitoring misuse, mechanisms to monitor how a system learns from feedback over time, improving the efficiency and accessibility of ML).

## 11. Safeguards

Question: Does the paper describe safeguards that have been put in place for responsible release of data or models that have a high risk for misuse (e.g., pretrained language models, image generators, or scraped datasets)?

Answer: [NA]

Justification: The paper poses no such risks.

Guidelines:

- The answer NA means that the paper poses no such risks.
- Released models that have a high risk for misuse or dual-use should be released with necessary safeguards to allow for controlled use of the model, for example by requiring that users adhere to usage guidelines or restrictions to access the model or implementing safety filters.
- Datasets that have been scraped from the Internet could pose safety risks. The authors should describe how they avoided releasing unsafe images.
- We recognize that providing effective safeguards is challenging, and many papers do not require this, but we encourage authors to take this into account and make a best faith effort.

## 12. Licenses for existing assets

Question: Are the creators or original owners of assets (e.g., code, data, models), used in the paper, properly credited and are the license and terms of use explicitly mentioned and properly respected?

Answer: [Yes]

Justification: All code, models, and datasets mentioned in the text are appropriately cited with their original papers.

Guidelines:

- The answer NA means that the paper does not use existing assets.
- The authors should cite the original paper that produced the code package or dataset.
- The authors should state which version of the asset is used and, if possible, include a URL.
- The name of the license (e.g., CC-BY 4.0) should be included for each asset.

- For scraped data from a particular source (e.g., website), the copyright and terms of service of that source should be provided.
- If assets are released, the license, copyright information, and terms of use in the package should be provided. For popular datasets, [paperswithcode.com/datasets](https://paperswithcode.com/datasets) has curated licenses for some datasets. Their licensing guide can help determine the license of a dataset.
- For existing datasets that are re-packaged, both the original license and the license of the derived asset (if it has changed) should be provided.
- If this information is not available online, the authors are encouraged to reach out to the asset's creators.

### 13. New assets

Question: Are new assets introduced in the paper well documented and is the documentation provided alongside the assets?

Answer: [\[Yes\]](#)

Justification: New assets introduced in the paper, such as code, are well documented. The documentation is provided alongside the assets in the supplementary material.

Guidelines:

- The answer NA means that the paper does not release new assets.
- Researchers should communicate the details of the dataset/code/model as part of their submissions via structured templates. This includes details about training, license, limitations, etc.
- The paper should discuss whether and how consent was obtained from people whose asset is used.
- At submission time, remember to anonymize your assets (if applicable). You can either create an anonymized URL or include an anonymized zip file.

### 14. Crowdsourcing and research with human subjects

Question: For crowdsourcing experiments and research with human subjects, does the paper include the full text of instructions given to participants and screenshots, if applicable, as well as details about compensation (if any)?

Answer: [\[NA\]](#)

Justification: The paper does not involve crowdsourcing nor research with human subjects.

Guidelines:

- The answer NA means that the paper does not involve crowdsourcing nor research with human subjects.
- Including this information in the supplemental material is fine, but if the main contribution of the paper involves human subjects, then as much detail as possible should be included in the main paper.
- According to the NeurIPS Code of Ethics, workers involved in data collection, curation, or other labor should be paid at least the minimum wage in the country of the data collector.

### 15. Institutional review board (IRB) approvals or equivalent for research with human subjects

Question: Does the paper describe potential risks incurred by study participants, whether such risks were disclosed to the subjects, and whether Institutional Review Board (IRB) approvals (or an equivalent approval/review based on the requirements of your country or institution) were obtained?

Answer: [\[NA\]](#)

Justification: The paper does not involve crowdsourcing nor research with human subjects.

Guidelines:

- The answer NA means that the paper does not involve crowdsourcing nor research with human subjects.

- 922 • Depending on the country in which research is conducted, IRB approval (or equivalent)  
923 may be required for any human subjects research. If you obtained IRB approval, you  
924 should clearly state this in the paper.
- 925 • We recognize that the procedures for this may vary significantly between institutions  
926 and locations, and we expect authors to adhere to the NeurIPS Code of Ethics and the  
927 guidelines for their institution.
- 928 • For initial submissions, do not include any information that would break anonymity (if  
929 applicable), such as the institution conducting the review.

#### 930 16. **Declaration of LLM usage**

931 Question: Does the paper describe the usage of LLMs if it is an important, original, or  
932 non-standard component of the core methods in this research? Note that if the LLM is used  
933 only for writing, editing, or formatting purposes and does not impact the core methodology,  
934 scientific rigorousness, or originality of the research, declaration is not required.

935 Answer: [NA]

936 Justification: The core method development in this research does not involve LLMs as any  
937 important, original, or non-standard components.

938 Guidelines:

- 939 • The answer NA means that the core method development in this research does not  
940 involve LLMs as any important, original, or non-standard components.
- 941 • Please refer to our LLM policy (<https://neurips.cc/Conferences/2025/LLM>)  
942 for what should or should not be described.